Revealing the photochemical activity of fluorographene towards organic transformations: Selective aerobic photooxidation of sulfides to sulfoxides

Alessandro Tabussi[a], Stamatis K. Serviou[a], Miroslav Medveď[b,c], Vítězslav Hrubý[b], Juraj Filo[d], Petr Lazar[b], Marek Cigáň[d], Demetrios D. Chronopoulos[a]*, Michal Otyepka[b,e], Christoforos G. Kokotos[a]*

[a] Laboratory of Organic Chemistry, Department of Chemistry, National and Kapodistrian University of Athens, Panepistimiopolis, Athens 15771, Greece

[b] Regional Centre of Advanced Technologies and Materials, Czech Advanced Technology and Research Institute (CATRIN), Palacký University Olomouc, Olomouc 779 00, Czech Republic

[c] Department of Chemistry, Faculty of Natural Sciences, Matej Bel University, Tajovského 40, 974 01 Banská Bystrica, Slovakia

[d] Department of Organic Chemistry, Faculty of Natural Sciences, Comenius University Bratislava, Ilkovičová 6, 842 15 Bratislava, Slovakia

[e] IT4Innovations, VŠB −Technical University of Ostrava, Ostrava-Poruba 708 00, Czech Republic

SUPPORTING INFORMATION

General Remarks

Chromatographic purification of the products was accomplished using forced-flow chromatography on Merck® Kieselgel 60 70-230 mesh. Thin-layer chromatography (TLC) was performed on aluminium-backed silica plates (0.2 mm, 60 F^{254}). Visualization of the developed chromatogram was performed using fluorescence quenching with phosphomolybdic acid, anisaldehyde, or potassium permanganate stains. Melting points were determined on a Buchi® 530 hot stage apparatus and are uncorrected. Mass spectra (ESI) were recorded on a Finningan® Surveyor MSQ LC-MS spectrometer. HRMS spectra were recorded on a Bruker® Maxis Impact QTOF spectrometer. ^{1}H-NMR and ^{13}C-NMR spectra were recorded on a Varian® Mercury (200 MHz, 188 MHz and 50 MHz, respectively) or on an Avance III HD Bruker 400 MHz (400 MHz, 376 MHz and 100 MHz, respectively) and are internally referenced to residual solvent signals. Data for ^{1}H-NMR are reported as follows: chemical shift (δ ppm), integration, multiplicity (s = singlet, d = doublet, t = triplet, q = quartet, m = multiplet, br s = broad signal), coupling constant, and assignment. Data for ^{13}C-NMR are reported in terms of chemical shift (δ ppm). Mass spectra and conversions of the reactions were recorded on a Shimadzu® GC-MS-QP2010 Plus Gas Chromatograph Mass Spectrometer utilizing a MEGA® column (MEGA-5, F.T.: 0.25 μm, I.D.: 0.25 mm, L.: 30 m, T_{max}: 350 ^{o}C, Column ID# 11475). FT-IR spectra were recorded on an iS5 FTIR spectrometer (Thermo Nicolet) using the Smart Orbit ZnSe ATR accessory. Briefly, a droplet of an aqueous dispersion of the relevant material was placed on a ZnSe crystal and left to dry and form a film. Spectra were acquired by summing 32 scans recorded under a nitrogen gas flow through the ATR accessory. ATR and baseline correction were applied to the collected spectra. X-ray photoelectron spectroscopy (XPS) was carried out with a Nexsa G2 XPS system (Thermo Scientific) spectrometer using an Al Kα source (hν = 1486.6 eV). The obtained data were evaluated using Avantage software (version 6.8.1). Deconvolution of HR-XPS spectra was performed in MagicPlot after Shirley background subtraction in OriginPro. Solid-state nuclear magnetic resonance (NMR) spectra were acquired using a JEOL spectrometer JNM-ECZ400R with a magnetic field of 9.4 T (working frequency 399.8 MHz for ^{1}H-NMR, 376.3 MHz for ^{19}F-NMR, and 100.5 MHz for ^{13}C-NMR). All the measurements were conducted at 18 kHz magic angle spinning (MAS) frequency using a 3.2 mm MAS probe. ^{19}F-NMR spectra were acquired using a single pulse TOSS (total suppression of spinning sidebands)

technique with a relaxation delay of 5 s. The ^{19}F-NMR chemical shift values were referenced to $CFCl_3$. Phase corrections involving both zero-order and first-order adjustments were applied to all spectra using Delta 6.1.0 software (JEOL). Additional baseline corrections were applied using OriginPro software. The deconvolution of all the spectra was conducted using MagicPlot software. UV-Vis absorption spectra were collected on a Cary 50 UV-Vis spectrophotometer (Varian). Transition electron microscopy images were obtained with a JEOL 2010 TEM equipped with a LaB6 type emission gun operating at 160 kV. AFM images were obtained in the amplitude modulated semicontact mode on an NT-MDT NTegra system equipped with a VIT-P AFM probe with the amplitude set point set to 71% of the free amplitude, a scanning speed of 0.5 Hz per line for all pictures, and using fresh cleaved muscovite mica.

Optimization of the Photochemical Aerobic Oxidation of Thioanisole (1a)

Catalyst Investigation

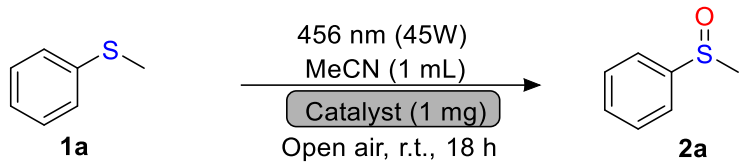

Table S1

Entry	Catalyst	Conversion (%)
1[a]	-	7
2	FG	33
3[b]	FG	-
4[c]	FG	35
5	Graphene	-
6	SWCNTs	3
7	MWCNTs	5
8	GCN	4

The reaction was performed with thioanisole (**1a**) (25 mg, 0.20 mmol), catalyst (1 mg) in MeCN (1 mL), under Blue LED irradiation (Kessil PR160L, 456 nm). FG was obtained after 30 minutes of sonication of GrF (1 mg) in the reaction's solvent, before the addition of **1a**. The rest of the materials were sonicated for 30 minutes in the reaction's solvent, before the addition of **1a**. Conversion was determined by ^{1}H-NMR. [a] The reaction was performed in the absence of a photocatalyst. [b] The reaction was performed without irradiation. [c] The reaction was performed by using 2 mg of GrF for producing FG. Graphene powder, single-walled (SW)CNTs, and multi-walled (MW)CNTs were purchased from Nanostructured & Amorphous Materials Inc. Cyanographene (GCN) was synthesized according to the reported procedure.[1]

Solvent Screening

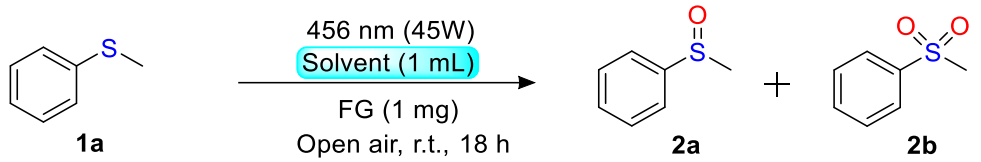

Table S2

Entry	Solvent	Conversion (%)	
		2a	**2b**
1	MeCN	33	2
2	MeOH	96 (75)	-
3	Ethyl acetate	5	-
4	CH_2Cl_2	18	3
5	DMSO	3	-
6	DMF	3	-
7	Petroleum ether	4	1
8	H_2O	2	-
9	THF	88	12
10	Cyrene	92	8

The reaction was performed with thioanisole (**1a**) (25 mg, 0.20 mmol), FG (1 mg) in solvent (1 mL), under Blue LED irradiation (Kessil PR160L, 456 nm). FG was obtained after 30 minutes of sonication of GrF in reaction's solvent, before the addition of **1a**. Conversions were determined by ^{1}H-NMR. Yield of **2a** after isolation by column chromatography is shown in parenthesis.

Irradiation Source Screening

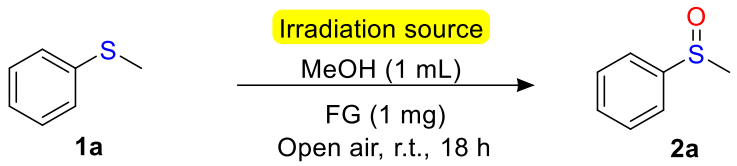

Table S3

Entry	Irradiation source (nm)	Conversion (%)
1	440	75
2	456	96 (75)
3	467	73
4	525	40
5	CFL	13

The reaction was performed with thioanisole (**1a**) (25 mg, 0.20 mmol), FG (1 mg) in solvent (1 mL), under irradiation. FG was obtained after 30 minutes of sonication of GrF (1 mg) in the reaction's solvent, before the addition of **1a**. Conversion was determined by ^{1}H-NMR. Yield of **2a** after isolation by column chromatography is shown in parentheses.

Ratio of FG/MeOH

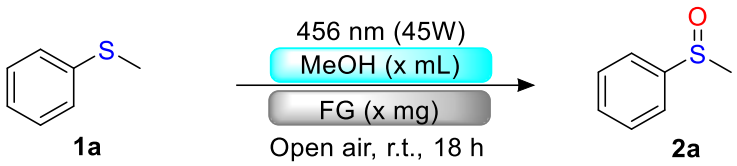

Table S4

Entry	mg of FG/ mL of MeOH	Conversion (%)
1	1 mg/ 1.0 mL	96 (75)
2	1 mg/ 0.5 mL	100 (92)
3	1 mg/ 2.0 mL	98 (79)
4	2 mg/ 1.0 mL	99 (95)

The reaction was performed with phenyl methyl sulfide (**1a**) (25 mg, 0.2 mmol), the corresponding ratio of FG/MeOH, under blue LED irradiation (Kessil PR160L, 456 nm). FG was obtained after 30 minutes of sonication of GrF in reaction's solvent, before the addition of **1a**. Conversion was determined by ^{1}H-NMR. Yield of **2a** after isolation by column chromatography is shown in parentheses.

Control Experiments

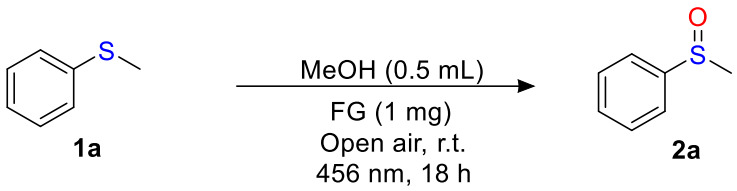

Table S5

Entry	Deviation from standard conditions	Conversion (%)
1	No sonication	27
2	No irradiation	-
3	No catalyst	14
4	Argon atmosphere	17
5	Dark, 60 °C	3

FG was obtained after 30 minutes of sonication of GrF in reaction's solvent, before the addition of **1a**. Conversion was determined by ^{1}H-NMR.

General Procedure for the Synthesis of Starting Materials

General Procedure for the Synthesis of Aryl-Alkyl Sulfides

The corresponding thiol (10.00 mmol) was dissolved in methanol (33 mL), followed by the addition of sodium methoxide (864 mg, 12.00 mmol), and the reaction mixture was cooled at -10 °C. The reaction mixture was stirred for 15 min at -10 °C, and then the corresponding bromide (12.00 mmol) was added slowly. After stirring for 18 h at room temperature, the solvent was removed *in vacuo*. The crude residue was diluted with water (100 mL) and extracted with chloroform (3 x 80 mL), the combined organic layers were washed with aq. NaOH 1N (1 x 80 mL) and brine (1 x 80 mL). The combined organic layers were dried (Na2SO4) and the solvent was removed *in vacuo*. The desired sulfide was isolated by column chromatography (Eluent: petroleum ether/ ethyl acetate 100:0).

General Procedure for the Synthesis of Alkyl-Alkyl Sulfides

The corresponding thiol (10.00 mmol) was dissolved in dry dimethylformamide (6.00 mL), followed by the addition of potassium carbonate (1.65 g, 12.00 mmol) and the reaction mixture was cooled at -10 °C. The reaction mixture was stirred for 15 min at -10 °C and then the corresponding bromide (12.00 mmol) was added slowly. After stirring for 18 h at room temperature, the reaction mixture was filtered and the solvent was removed *in vacuo*. The desired sulfide was isolated by column chromatography. Eluent: petroleum ether/ ethyl acetate 100:0).

Methyl(phenyl)sulfide (1a)[2]

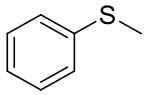

Colorless oil; (**80**%); Eluent: Petroleum Ether / Ethyl Acetate 100:0; NMR data in accordance with reported literature.[2]

^{1}H NMR (400 MHz, $CDCl_3$) δ: 7.35-7.31 (4H, m, ArH), 7.20-7.18 (1H, m, ArH), 2.52 (3H, s, SCH_3); **^{13}C NMR** (100 MHz, $CDCl_3$) δ: 138.4, 128.8, 126.6, 125.0, 15.8; **MS (ESI)** m/z 125 $[M+H]^+$.

Butyl(phenyl)sulfide (1b)[3]

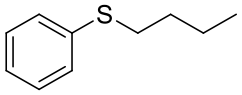

Colorless oil; (**81**%); Eluent: Petroleum Ether / Ethyl Acetate 100:0; NMR data in accordance with reported literature.[3]

^{1}H NMR (400 MHz, $CDCl_3$) δ: 7.33 (4H, m, ArH), 7.19 (1H, t, J = 7.1 Hz, ArH), 2.95 (2H, t, J = 7.4 Hz, SCH_2), 1.71-1.62 (2H, m, CH_2), 1.49 (2H, sext, J = 7.4 Hz, CH_2), 0.95 (3H, t, J = 7.3 Hz, CH_3); **^{13}C NMR** (100 MHz, $CDCl_3$) δ: 137.06, 128.86, 125.64, 33.27, 31.24, 21.98, 13.65. **MS (ESI)** m/z 167 $[M+H]^+$.

Octyl(phenyl)sulfide (1c)[4]

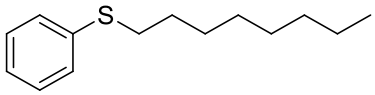

Colorless oil; (**57**%); Eluent: Petroleum Ether / Ethyl Acetate 100:0; NMR data in accordance with reported literature.[4]

^{1}H NMR (400 MHz, $CDCl_3$) δ: 7.32 (2H, d, J = 7.8 Hz, ArH), 7.27 (2 H, t, J = 7.8 Hz, ArH), 7.16 (1H, t, J = 7.8 Hz, ArH), 2.92 (2H, t, J = 7.2 Hz, SCH_2), 1.64 (2H, q, J = 7.0 Hz, CH_2), 1.46-1.38 (2H, m, CH_2), 1.36-1.28 (8H, m, 4 x CH_2), 0.88 (3H, t, J = 7.0 Hz, CH_3); **^{13}C NMR** (100 MHz, $CDCl_3$) δ: 137.1, 128.9, 128.8, 128.6, 33.6, 31.8, 29.2, 29.2, 29.1, 28.9, 22.7, 14.1; **MS (ESI)** m/z 223 $[M+H]^+$.

Cyclopentyl(phenyl)sulfide (1d)[2]

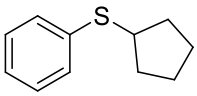

Colorless oil; (**71**%); Eluent: Petroleum Ether / Ethyl Acetate 100:0; NMR data in accordance with reported literature.[2]

^{1}H NMR (400 MHz, $CDCl_3$) δ: 7.39 (2H, d, J = 7.3 Hz, ArH), 7.30 (2H, t, J = 7.3 Hz, ArH), 7.20 (1H, t, J = 7.3 Hz, ArH), 3.66-3.58 (1H, m, SCH), 2.12-2.06 (2H, m, 2 x CH*H*), 1.81-1.79 (2H, m, 2 x CH*H*), 1.67-1.59 (4H, m, 4 x CH*H*); **^{13}C NMR** (100 MHz, $CDCl_3$) δ: 137.3, 129.9, 128.7, 125.8, 45.9, 33.5, 24.8; **MS (ESI)** m/z 179 $[M+H]^+$.

Allyl(phenyl)sulfide (1e)[2]

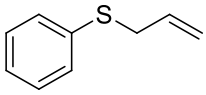

Colorless oil; (**90%**); Eluent: Petroleum ether / Ethyl acetate 100:0; NMR data in accordance with reported literature.[2]

^{1}H NMR (400 MHz, $CDCl_3$) δ: 7.38 (2H, d, J = 7.5 Hz, ArH), 7.31 (2H, t, J = 7.5 Hz, ArH), 7.22 (1H, t, J = 7.5 Hz, ArH), 5.92 (1H, ddt, J = 16.9, 10.0 and 6.9 Hz, CH), 5.17 (1H, d, J = 16.9 Hz, C*H*H), 5.11 (1H, d, J = 10.0 Hz, CH*H*), 3.59 (2H, d, J = 6.9 Hz, SCH_2); **^{13}C NMR** (100 MHz, $CDCl_3$) δ: 135.9, 133.6, 129.8, 128.8, 126.2, 117.6, 37.1; **MS (ESI)** m/z 151 $[M+H]^+$.

Propargyl(phenyl)sulfide (1f)[2]

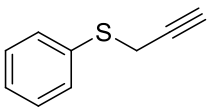

Yellowish oil; (**55%**); Eluent: Petroleum ether / Ethyl acetate 100:0; NMR data in accordance with reported literature.[2]

^{1}H NMR (400 MHz, $CDCl_3$) δ: 7.49 (2H, d, J = 7.7 Hz, ArH), 7.36 (2H, t, J = 7.7 Hz, ArH), 7.31-7.28 (1H, m, ArH), 3.64 (2H, d, J = 2.6 Hz, CH_2), 2.27 (1H, t, J = 2.6 Hz, ≡CH); **^{13}C NMR** (100 MHz, $CDCl_3$) δ: 134.9, 130.1, 129.0, 126.9, 79.8, 71.5, 22.5; **MS (ESI)** m/z 149 $[M+H]^+$.

2-(Phenylthio)ethan-1-ol (1g)[2]

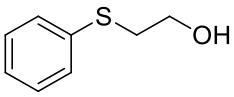

Colorless oil; (**76**%); Eluent: Petroleum Ether / Ethyl Acetate 98:2; NMR data in accordance with reported literature.[2]

^{1}H NMR (400 MHz, $CDCl_3$) δ: 7.42 (2H, d, J = 7.4 Hz, ArH), 7.32 (2H, t, J = 7.4 Hz, ArH), 7.25 (1H, t, J = 7.4 Hz, ArH), 3.77 (2H, t, J = 5.8 Hz, OCH_2), 3.14 (2H, t, J = 5.8 Hz, SCH_2), 2.10 (1H, br s, OH); **^{13}C NMR** (100 MHz, $CDCl_3$) δ: 134.9, 129.9, 128.8, 126.5, 60.3, 36.9; **MS (ESI)** m/z 155 $[M+H]^+$.

Ethyl-3-(phenylthio)propanoate (1h)[2]

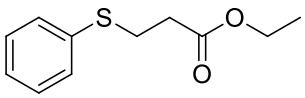

Yellowish oil; (**23**%); Eluent: Petroleum Ether / Ethyl Acetate 98:2; NMR data in accordance with reported literature.[2]

^{1}H NMR (400 MHz, $CDCl_3$) δ: 7.40 (2H, d, J = 7.6 Hz, ArH), 7.32 (2H, t, J = 7.6 Hz, ArH), 7.23 (1H, t, J = 7.6 Hz, ArH), 4.16 (2H, q, J = 7.1 Hz, OCH_2), 3.19 (2H, t, J = 7.4 Hz,bSCH_2), 2.64 (2H, t, J = 7.4 Hz, CH_2), 1.28 (3H, t, J = 7.1 Hz, CH_3);**^{13}C NMR** (100 MHz, $CDCl_3$) δ: 171.8, 135.3, 130.1, 129.0, 126.5, 60.7, 34.5, 29.1, 14.2; **MS (ESI)** m/z 211 $[M+H]^+$.

Dodecyl(methyl)sulfide (1i)[2]

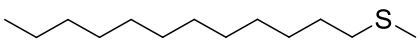

Colorless oil; (**82**%); Eluent: Petroleum Ether 100%; NMR data in accordance with reported literature.[2]

^{1}H NMR (400 MHz, $CDCl_3$) δ: 2.51 (2H, t, J = 7.4 Hz, SCH_2), 2.12 (3H, s, SCH_3), 1.66-1.58 (2H, m, CH_2), 1.44-1.38 (2H, m, CH_2), 1.34-1.22 (16H, m, 8 x CH_2), 0.90 (3H, t, J = 6.4 Hz, CH_3); **^{13}C NMR** (100 MHz, $CDCl_3$) δ: 34.3, 31.9, 29.6, 29.6, 29.6, 29.5, 29.3, 29.2, 29.2, 28.8, 22.6, 15.5, 14.0; **MS (ESI)** m/z 217 $[M+H]^+$.

Butyl(dodecyl)sulfide (1j)[2]

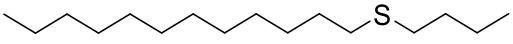

Colorless oil; (**40**%); Eluent: Petroleum Ether 100%; NMR data in accordance with reported literature.[2]

^{1}H NMR (400 MHz, $CDCl_3$) δ: 2.55-2.49 (4H, m, 2 x SCH_2), 1.64-1.54 (4H, m, 2 x CH_2), 1.48-1.35 (4H, m, 2 x CH_2), 1.36-1.24 (16H, m, 8 x CH_2), 0.97-0.87 (6H, m, 2 x CH_3); **^{13}C NMR** (100 MHz, $CDCl_3$) δ: 32.2, 31.9, 31.9, 31.8, 29.7, 29.7, 29.6, 29.6, 29.5, 29.4, 29.3, 29.0, 22.7, 22.1, 14.1, 13.7; **HRMS** calculated for $C_{16}H_{35}S^+$ $[M+H^+]$: 259.2454, found: 259.2456.

Benzyl(methyl)sulfide (1k)[2]

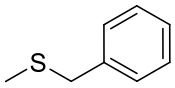

Colorless oil; (**56%**); Eluent: Petroleum ether / Ethyl acetate 100:0; NMR data in accordance with reported literature.[2]

^{1}H NMR (400 MHz, $CDCl_3$) δ: 7.43-7.24 (5H, m, ArH), 3.73 (2H, s, SCH_2), 2.05 (3H, s, SCH_3); **^{13}C NMR** (100 MHz, $CDCl_3$) δ: 138.2, 128.7, 128.3, 126.8, 38.2, 14.8; **MS (ESI)** m/z 139 $[M+H]^+$.

Benzyl(cyclohexyl)sulfide (1l)[2]

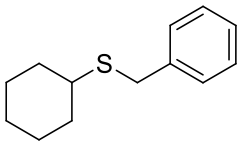

Colorless oil; (**90%**); Eluent: Petroleum ether / Ethyl acetate 100:0; NMR data in accordance with reported literature.[2]

^{1}H NMR (400 MHz, $CDCl_3$) δ: 7.38-7.29 (5H, m, ArH), 3.78 (2H, s, SCH_2), 2.66-2.56 (1H, m, SCH), 2.00-1.94 (2H, m, 2 x CH*H*), 1.83-1.73 (2H, m, 2 x CH*H*), 1.66-1.57 (1H, m, C*H*H), 1.44-1.23 (5H, m, 5 x CH*H*); **^{13}C NMR** (100 MHz, $CDCl_3$) δ: 138.9, 128.7, 128.4, 126.7, 42.9, 34.6, 33.3, 25.9, 25.8; **MS (ESI)** m/z 125 $[M+H]^+$.

General Procedure for the Photochemical Aerobic Oxidation of Sulfides to Sulfoxides

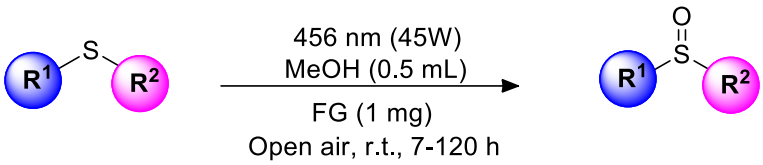

In a glass vial containing graphite fluoride (GrF) (1 mg), methanol was added (0.5 mL), and then, the suspension was sonicated for 30 min. Eventually, the corresponding sulfide (0.20 mmol) was added into the solution and the reaction mixture was left stirring under blue LED irradiation (Kessil PR160L, 456 nm) for 7-120 h. The reaction mixture was filtered, and the solvent removed *in vacuo*. The desired sulfoxide was isolated by column chromatography (eluent: petroleum ether/ethyl acetate: 7/3 to $CHCl_3$/ MeOH : 9/1).

(Methylsulfinyl)benzene (2a)[2]

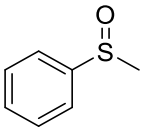

Colorless oil; 18 h; (**92%**); Eluent: Petroleum ether / Ethyl acetate 60:40; NMR data in accordance with reported literature.[2]

^{1}H NMR (400 MHz, $CDCl_3$) δ: 7.66-7.64 (2H, m, ArH), 7.55-7.50 (3H, m, ArH), 2.72 (3H, s, SCH_3); **^{13}C NMR** (100 MHz, $CDCl_3$) δ: 145.7, 131.0, 129.3, 123.5, 43.9; **MS (ESI)** m/z 141 $[M+H]^+$.

(Butylsulfinyl)benzene (2b)[5]

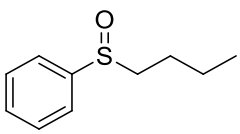

Colorless oil; 24 h; (**96%**); Eluent: Petroleum ether / Ethyl acetate 60:40; NMR data in accordance with reported literature.[5]

^{1}H NMR (400 MHz, $CDCl_3$) δ: 7.60 (2H, d, *J* = 7.0 Hz, ArH), 7.53-7.44 (3H, m, ArH), 2.77 (2H, m, SCH_2), 1.77-1.65 (1H, m, C*H*H), 1.63-1.51 (1H, m, C*H*H), 1.49-1.33 (2H, m, CH_2), 0.89 (3H, t, *J* = 7.3 Hz, CH_3); **^{13}C NMR** (100 MHz, $CDCl_3$) δ: 144.1, 131.0, 129.3, 124.1, 57.1, 24.2, 22.0, 13.7; **MS (ESI) m/z** 205 $[M+Na]^+$.

(Octylsulfinyl)benzene (2c)[6]

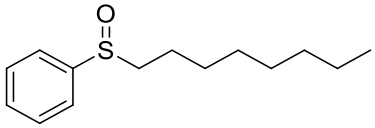

Colorless oil; 18 h; (**93%**); Eluent: Petroleum ether / Ethyl acetate 60:40; NMR data in accordance with reported literature.[6]

^{1}H NMR (400 MHz, CDCl3) δ: 7.60 (2H, d, *J* = 7.1 Hz, ArH), 7.54-7.44 (3H, m, ArH), 2.77 (2H, m, SCH_2), 1.79-1.66 (1H, m, C*H*H), 1.65-1.54 (1H, m, C*H*H), 1.46-1.32 (2H, m, 2 x C*H*H), 1.31-1.17 (8H, m, 8 x C*H*H), 0.85 (3H, t, *J* = 6.7 Hz, CH_3); **^{13}C NMR** (100 MHz, CDCl3) δ: 144.2, 131.0, 129.3, 124.1, 57.5, 31.8, 29.2, 29.1, 28.7, 22.7, 22.2, 14.1; **MS (ESI)** m/z 239 $[M+Na]^+$.

(Cyclopentylsulfinyl)benzene (2d)[2]

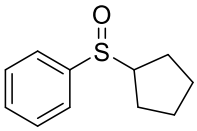

Yellow oil; 18h; (**97%**); Eluent: Petroleum ether / Ethyl acetate 60:40; NMR data in accordance with reported literature.[2]

^{1}H NMR (400 MHz, $CDCl_3$) *δ*: 7.63-7.61 (2H, m, ArH), 7.51-7.44 (3H, m, ArH), 3.09 (1H, quint, *J* = 7.5 Hz, SCH), 2.10-2.04 (1H, m, C*H*H), 1.82-1.77 (2H, m, 2 x C*H*H), 1.73-1.56 (5H, m, 5 x C*H*H); **^{13}C NMR** (100 MHz, $CDCl_3$) *δ*: 143.5, 130.7, 128.8, 124.4, 64.2, 27.5, 25.9, 25.5, 24.7; **MS (ESI)** m/z 195 $[M+H]^+$.

(Allylsulfinyl)benzene (2e)[2]

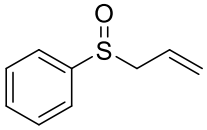

Colorless oil; 48 h; (**40%**); Eluent: Petroleum ether / Ethyl acetate 60:40; NMR data in accordance with reported literature.[2]

^{1}H NMR (400 MHz, $CDCl_3$) δ: 7.61-7.59 (2H, m, ArH), 7.52-7.51 (3H, m, ArH), 5.65 (1H, ddt, *J* = 17.1 Hz, 10.2 Hz and 7.5 Hz, =CH), 5.33 (1H, d, *J* =10.2 Hz, =C*H*H), 5.20 (1H, d, *J* =17.1 Hz, =C*H*H), 3.58 (1H, dd, *J* = 12.9 Hz and 7.5 Hz, SC*H*H), 3.51 (1H, dd, *J* = 12.9 Hz and 7.5 Hz, SC*H*H); **^{13}C NMR** (100 MHz, $CDCl_3$) δ: 143.0, 131.1, 129.0, 125.3, 124.4, 123.9, 60.9; **MS (ESI)** m/z 167 $[M+H]^+$.

(Prop-2-yn-1-ylsulfinyl)benzene (2f)[2]

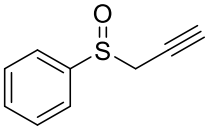

Yellowish oil; 48 h; (**42%**); Eluent: Petroleum ether / Ethyl acetate 60:40; NMR data in accordance with reported literature.[2]

^{1}H NMR (400 MHz, $CDCl_3$) δ: 7.73-7.71 (2H, m, ArH), 7.56-7.54 (3H, m, ArH), 3.69 (1H, d, *J* =15.5 Hz, SC*H*H), 3.63 (1H, d, *J* =15.5 Hz, SC*H*H), 2.34 (1H, s, ≡CH); **^{13}C NMR** (100 MHz, $CDCl_3$) δ: 142.7, 131.8, 129.1, 124.5, 76.4, 72.7, 47.7; **MS (ESI)** m/z 165 $[M+H]^+$.

3-(Phenylsulfinyl)ethanol (2g)[2]

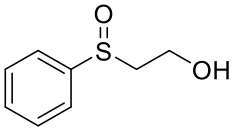

Yellowish oil; 48 h; (**93%**); Eluent: $CHCl_3$ / MeOH 90:10; NMR data in accordance with reported literature.[2]

^{1}H NMR (400 MHz, $CDCl_3$) δ: 7.63 (2H, d, *J* = 7.0 Hz, ArH), 7.54-7.47 (3H, m, ArH), 4.18-4.12 (1H, m, OC*H*H), 3.99-3.94 (2H, m, OCH*H* and O*H*), 3.12 (1H, dd, *J* = 13.6 Hz and 4.5 Hz, SC*H*H), 2.91 (1H, dd, *J* = 13.6 Hz and 4.5 Hz, SC*H*H); **^{13}C NMR** (100 MHz, $CDCl_3$) δ: 143.0, 131.2, 129.4, 123.9, 58.3, 57.0; **MS (ESI)** m/z 171 $[M+H]^+$.

Ethyl-3-(phenylsulfinyl)propanoate (2h)[2]

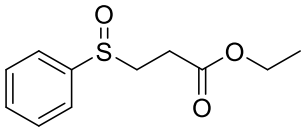

Yellowish oil; 18 h; (**48%**); Eluent: Petroleum ether / Ethyl acetate: 98:2; NMR data in accordance with reported literature.[2]

^{1}H NMR (400 MHz, $CDCl_3$) *δ*: 7.62-7.56 (2H, m, ArH), 7.53-7.51 (3H, m, ArH), 4.10 (2H, q, *J* = 7.2 Hz, OCH_2), 3.23 (1H, ddd, *J* = 13.7, 8.5 and 6.9 Hz, C*H*H), 2.97 (1H, ddd, *J* = 13.7, 8.5 and 5.8 Hz, C*H*H), 2.82 (1H, ddd, *J* = 16.9, 8.5 and 6.9 Hz, C*H*H), 2.53 (1H, ddd, *J* = 16.9, 8.5 and 5.8 Hz, CH*H*), 1.23 (3H, t, *J* = 7.2 Hz, CH_3); **^{13}C NMR** (100 MHz, $CDCl_3$) *δ*: 171.1, 142.9, 131.1, 129.2, 124.0, 61.0, 51.1, 26.1, 14.0; **MS (ESI)** m/z 199 $[M+H]^+$.

3-(Phenylsulfinyl)propanoic acid (2i)[2]

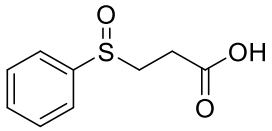

White solid; m.p.: 95-97 ºC; 48 h; (**50**%); Eluent: $CHCl_3$/MeOH 90:10; NMR data in accordance with reported literature.[2]

^{1}H NMR (400 MHz, CD_3OD) δ: 7.73-7.70 (2H, m, ArH), 7.64-7.58 (3H, m, ArH), 3.25 (1H, dt, *J* = 14.4 and 7.1 Hz, COC*H*H), 3.10 (1H, dt, *J* = 14.4 and 7.1 Hz, COC*H*H), 2.64, (1H, dt, *J* = 16.5 and 7.1 Hz, SC*H*H), 2.41 (1H, dt, *J* = 16.5 and 7.1 Hz, SC*H*H); **^{13}C NMR** (100 MHz, CD_3OD) δ: 177.8, 143.9, 132.6, 130.6, 125.4, 54.1, 30.0; **MS (ESI)** m/z 199 $[M+H]^+$.

1-(Methylsulfinyl)dodecane (2j)[2]

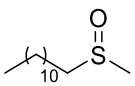

White solid; m.p.: 62-64 ºC; 18 h; (**62%**); Eluent: Petroleum ether / Ethyl acetate 60:40; NMR data in accordance with reported literature.[2]

^{1}H NMR (400 MHz, $CDCl_3$) *δ*: 2.75-2.68 (1H, m, SC*H*H), 2.66-2.59 (1H, m, SC*H*H), 2.54 (1H, s, SCH_3), 1.73 (2H, quint, *J* = 6.6 Hz, CH_2), 1.46-1.24 (18H, m, 9 x CH_2), 0.86 (3H, t, *J* = 6.6 Hz, CH_3); **^{13}C NMR** (100 MHz, $CDCl_3$) *δ*: 54.8, 38.5, 31.9, 29.6, 29.5, 29.3, 29.3, 29.2, 28.8, 22.6, 22.5, 14.1; **MS (ESI)** m/z 121 $[M+H]^+$.

1-(Butylsulfinyl)dodecane (2k)

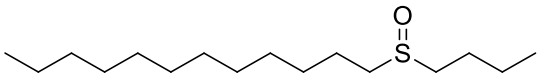

Colorless oil; 18 h; (**94%**); Eluent: Petroleum ether / Ethyl acetate 60:40.

^{1}H NMR (400 MHz, $CDCl_3$) δ 2.73-2.57 (4H, m, 4 x SCH*H*), 1.84-1.69 (4H, m, 4 x CH*H*), 1.54-1.37 (4H, m, 2 x CH_2), 1.39-1.19 (16H, m, 8 x CH_2), 0.96 (3H, t, *J* = 7.3 Hz, CH_3), 0.87 (3H, t, *J* = 6.5 Hz, CH_3); **^{13}C NMR** (100 MHz, $CDCl_3$) *δ*: 52.5, 52.2, 32.0, 29.7, 29.7, 29.6, 29.4, 29.4, 29.3, 29.0, 24.7, 22.7, 22.7, 22.2, 14.2, 13.8; **HRMS** calculated for $C_{16}H_{35}OS^+$ [M+H$^+$]: 275.2403, found: 275.2403.

Tetrahydrothiophene-1-oxide (2l)[2]

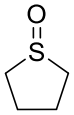

Colorless oil; 18 h; (**60%**); Eluent: Petroleum ether / Ethyl acetate 60:40; NMR data in accordance with reported literature.[2]

^{1}H NMR (400 MHz, $CDCl_3$) *δ*: 2.89-2.72 (4H, m, 2 x SCH_2), 2.45-2.33 (2H, m, 2 x CH_2), 2.03-1.90 (2H, m, 2 x CH_2); **^{13}C NMR** (100 MHz, $CDCl_3$) *δ*: 54.3, 25.3; **MS (ESI)** m/z 105 [M+H]$^+$.

Tetrahydro-*2H*-thiopyran-1-oxide (2m)[2]

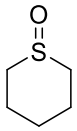

Colorless oil; 18 h; (**73%**); Eluent: Petroleum ether / Ethyl acetate 60:40; NMR data in accordance with reported literature.[2]

^{1}H NMR (400 MHz, $CDCl_3$) *δ*: 2.88 (2H, t, *J* = 10.9 Hz, 2 x SCH*H*), 2.76 (2H, t, *J* = 10.9 Hz, 2 x SCH*H*), 2.29-2.16 (2H, m, CH_2), 1.70-1.55 (4H, m, 2 x CH_2); **^{13}C NMR** (100 MHz, $CDCl_3$) *δ*: 48.9, 24.6, 19.1; **MS (ESI)** m/z 119 [M+H]$^+$.

(2S)-2-((*tert*-Butoxycarbonyl)amino)-4-(methylsulfinyl)butanoic acid (2n)[2]

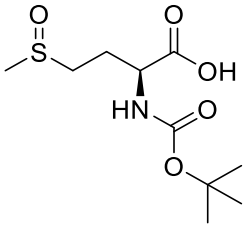

Pale yellow solid; m.p 114-116 ^{o}C; 40 h; (**32%**); Eluent: Petroleum ether / Ethyl acetate 60:40; Mixture of diastereomers. Eluent: Petroleum ether / Ethyl acetate 60:40; NMR data in accordance with reported literature.[2]

^{1}H NMR (400 MHz, CDCl3) δ: 8.27 (1H, br s, OH), 5.68-5.60 (1H, m, NH), 4.44-4.30 (1H, m, NCH), 2.95-2.86 (2H, m, SCH_2), 2.67 (1.5H, s, SCH_3), 2.63 (1.5H, s, SCH_3), 2.39-2.24 (1H, m, C*H*H), 2.22-2.00 (1H, m, C*H*H), 1.41 [9H, s, $C(CH_3)_3$]; **^{13}C NMR** (100 MHz, CDCl3) δ: 173.3, 173.3, 155.8, 155.7, 80.4, 52.6, 52.3, 49.5, 37.8, 37.5, 28.8, 28.4, 28.1, 26.4, 25.9; **MS (ESI)** m/z 266 $[M+H]^+$.

((Methylsulfinyl)methyl)benzene (2o)[2]

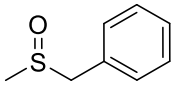

White solid; m.p.: 54-56 ^{o}C; 18 h; (**78%**); Eluent: Petroleum ether / Ethyl acetate 60:40; NMR data in accordance with reported literature.[2]

^{1}H NMR (400 MHz, $CDCl_3$) *δ*: 7.42-7.36 (3H, m, ArH), 7.31-7.29 (2H, m, ArH), 4.07 (1H, d, *J* = 12.8 Hz, SC*H*H), 3.94 (1H, d, *J* = 12.8 Hz, SCH*H*), 2.47 (3H, s, SCH_3); **^{13}C NMR** (100 MHz, $CDCl_3$) *δ*: 130.0, 129.6, 129.0, 128.4, 60.2, 37.2; **MS (ESI)** m/z 155 $[M+H]^+$.

((Cyclohexylsulfinyl)methyl)benzene (2p)[2]

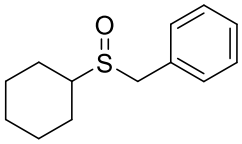

White solid; m.p.: 82-84 ^{o}C; 18 h; (**76%**); Eluent: Petroleum ether / Ethyl acetate 60:40; NMR data in accordance with reported literature.[2]

^{1}H NMR (400 MHz, $CDCl_3$) *δ*: 7.39-7.29 (5H, m, ArH), 3.98 (1H, d, *J* =13.1 Hz, SC*H*H), 3.89 (1H, d, *J* =13.1 Hz, SCH*H*), 2.49-2.43 (1H, m, SCH), 2.11-2.07 (1H, m, C*H*H), 1.95-1.84 (3H, m, 3 x C*H*H), 1.70-1.67 (1H, m, CH*H*), 1.57-1.49 (2H, m, 2 x C*H*H), 1.36-1.23

(3H, m, 3 x C*H*H); **^{13}C NMR** (100 MHz, $CDCl_3$) δ: 130.6, 129.9, 128.9, 128.1, 56.9, 54.7, 26.9, 25.4, 25.4, 25.1, 23.9; **MS (ESI)** m/z 223 $[M+H]^+$.

(Sulfinylbis(methylene))dibenzene (2q)[2]

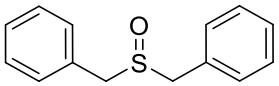

White solid; m.p.: 132-134 ºC; 48 h; (**83%**); Eluent: Petroleum ether / Ethyl acetate 60:40; NMR data in accordance with reported literature.[2]

^{1}H NMR (400 MHz, $CDCl_3$) δ: 7.40-7.32 (6H, m, ArH), 7.30-7.27 (4H, m, ArH), 3.92 (2H, d, *J* = 13.0 Hz, 2 x SC*H*H), 3.86 (2H, d, *J* = 13.0 Hz, 2 x SC*H*H); **^{13}C NMR** (100 MHz, $CDCl_3$) δ: 130.1, 130.0, 128.9, 128.3, 57.1; **MS (ESI)** m/z 231 $[M+H]^+$.

1-Bromo-4-((phenylsulfinyl)methyl)benzene (2r)[2]

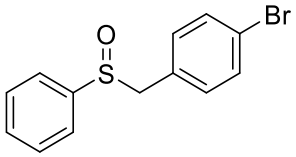

White solid; m.p.:177-179 ºC; 18 h; (**69%**); Eluent: Petroleum ether / Ethyl acetate 60:40; NMR data in accordance with reported literature.[2]

^{1}H NMR (400 MHz, $CDCl_3$) δ: 7.49-7.41 (3H, m, ArH), 7.37-7.35 (4H, m, ArH), 6.82 (2H, d, *J* = 7.0 Hz, ArH), 3.99 (1H, d, *J* =12.8 Hz, SC*H*H), 3.94 (1H, d, *J* =12.8 Hz, SC*H*H); **^{13}C NMR** (100 MHz, $CDCl_3$) δ: 142.3, 131.9, 131.5, 131.3, 129.0, 127.9, 124.4, 122.6, 62.5; **MS (ESI)** m/z 295 $[M+H]^+$.

Sulfinyldibenzene (2s)[2]

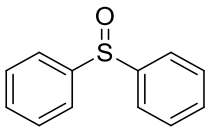

Colorless oil; 120 h; (**52%**); Eluent: Petroleum ether / Ethyl acetate 60:40. Eluent: Petroleum ether / Ethyl acetate 60:40; NMR data in accordance with reported literature.[2]

^{1}H NMR (400 MHz, CDCl3) δ: 7.66-7.61 (4H, m, ArH), 7.50-7.43 (6H, m, ArH); **^{13}C NMR** (100 MHz, CDCl3) δ: 145.0, 131.4, 129.5, 125.0; **MS (ESI)** m/z 203 $[M+H]^+$.

2-(Benzhydrylsulfinyl)acetamide (2t)[2]

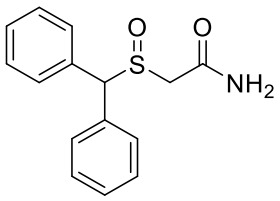

Colorless solid; m.p.: 158-160 ^{o}C; 7 h; (**40%**); Eluent: Petroleum ether / Ethyl acetate 50:50. Eluent: Petroleum ether / Ethyl acetate 60:40; NMR data in accordance with reported literature.[2]

^{1}H NMR (400 MHz, CDCl3) δ: 7.52-7.47 (2H, m, ArH), 7.46-7.33 (8H, m, ArH), 7.05 (1H, br s, N*H*H), 5.62, (1H, br, s, N*H*H), 5.20 (1H, s, SCH), 3.49 (1H, d, *J* = 14.3 Hz, SC*H*H), 3.10 (1H, d, *J* = 14.3 Hz, SC*H*H); **^{13}C NMR** (100 MHz, CDCl3) δ: 166.3, 134.5, 134.2, 129.6, 129.5, 129.1, 129.0, 129.0, 128.8, 71.8, 51.5; **MS (ESI)** m/z 273 $[M+H]^{+}$.

Quenching Studies on the Photochemical Aerobic Oxidation of Sulfides

In a glass vial containing the photocatalyst graphite fluoride (GrF) (1 mg), methanol (0.5 mL) was added. Then, the solution was sonicated for 30 min. Eventually, thioanisole (0.20 mmol) and quencher (0.20 mmol) were added to the solution and the reaction mixture was left stirring under blue LED irradiation (Kessil PR160L, 456 nm) for 18 h. The solution was filtered and the solvent removed *in vacuo*. Conversions were determined by ^{1}H-NMR.

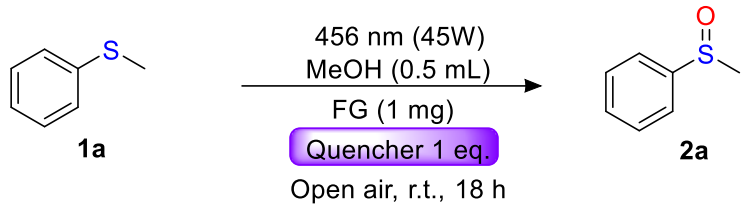

Table S6

Entry	Quencher	Conversion (%)	
1	1,4-Dimethoxybenzene	22	Radical
2	Hydroquinone	9	Radical
3	BHT	13	Radical
4	$CuSO_4$	30	Electron
5	KI	13	Hole
6	NaN_3	11	$^1O_2$
7	DABCO	14	$^1O_2$
8	p-Benzoquinone	19	$^{\bullet}O_2^-$
9	*t*-BuOH	97	$^{\bullet}OH$
10	-	100	

The reaction was performed with thioanisole (**1a**) (25 mg, 0.20 mmol), FG (1 mg) in MeOH (0.5 mL), under Blue LED irradiation (Kessil PR160L, 456 nm). FG was obtained after 30 minutes of sonication of GrF in reaction's solvent, before the addition of **1a** and quencher. Conversion was determined by ^{1}H-NMR.

UV-Vis Studies

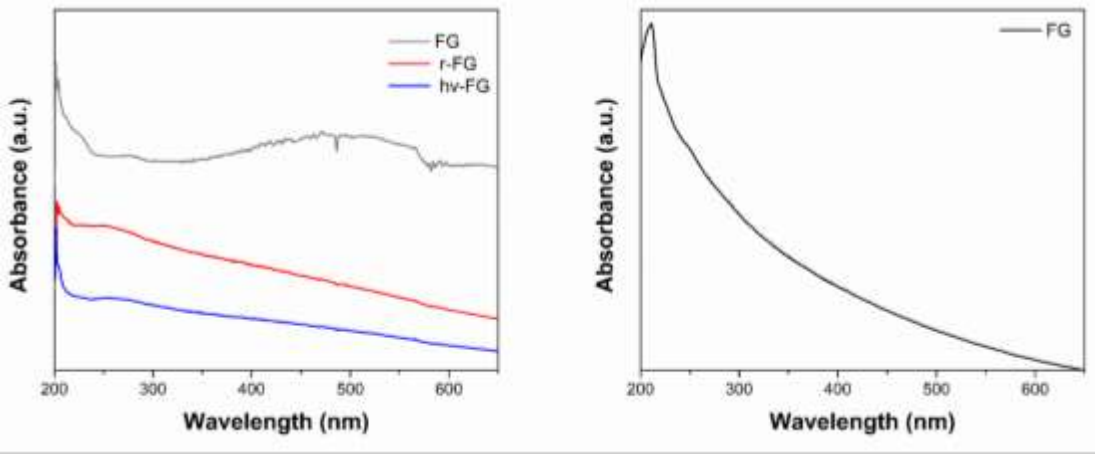

Figure S1. UV-Vis spectra of FG, r-FG and hv-FG in MeOH (left), and of FG in MeCN (right).

Hydrogen Peroxide Generation Detection Test

KI – glacial acetic acid solution preparation: 100 mg of potassium iodide were dissolved in 10 mL of glacial acetic acid.

Validation of the H_2O_2 detection utilizing commercially available H_2O_2: 0.5 mL of commercially available H_2O_2 was added to the KI-glacial acetic acid solution and the immediate change from a yellowish solution to a dark brown solution indicated the presence of H_2O_2 *(positive result)*.

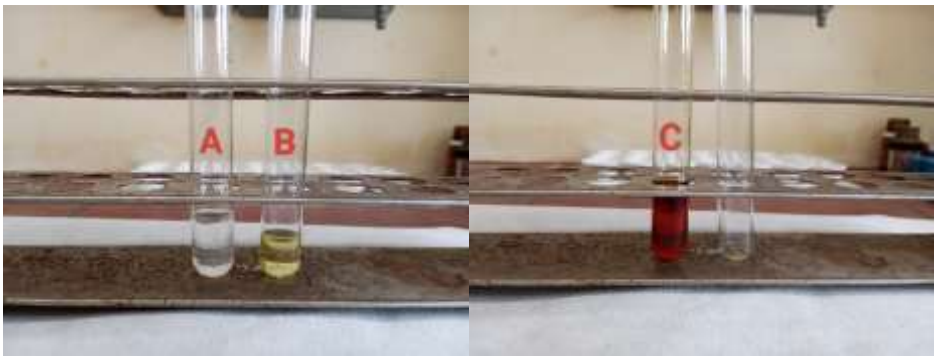

Figure S2. A) Commercially available H_2O_2, **B)** KI-glacial acetic acid solution, and **C)** resulting solution after mixture of **A** and **B** *(positive result)*.

Test for the detection of H_2O_2 in the irradiated reaction mixture: In a glass vial containing GrF (1 mg), methanol was added (0.5 mL) and then, the suspension was sonicated for 30 min. Eventually, thioanisole (1 eq., 0.20 mmol, 25 mg) was added into the suspension and the reaction mixture was left stirring under blue LED irradiation (Kessil PR160L, 456 nm) for 5 h. The irradiated reaction mixture was added to the KI – glacial acetic acid solution and no significant change in color was observed (*negative result*).

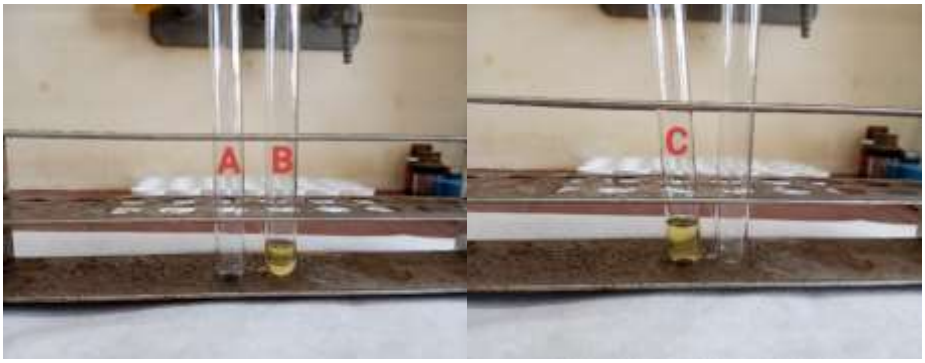

Figure S3. A) Irradiated reaction mixture, **B)** KI-glacial acetic acid solution, and **C)** resulting solution after mixture of **A** and **B** *(negative result)*.

Test for the detection of H_2O_2 in the non-irradiated reaction mixture: In a glass vial containing GrF (1 mg), methanol (0.5 mL) was added, and then the suspension was sonicated for 30 min. Eventually, thioanisole (1 eq., 0.20 mmol, 25 mg) was added to the suspension, and the reaction mixture was stirred for about an hour. The non-irradiated reaction mixture was added to the KI – glacial acetic acid solution and no significant change in color was observed (*negative result*).

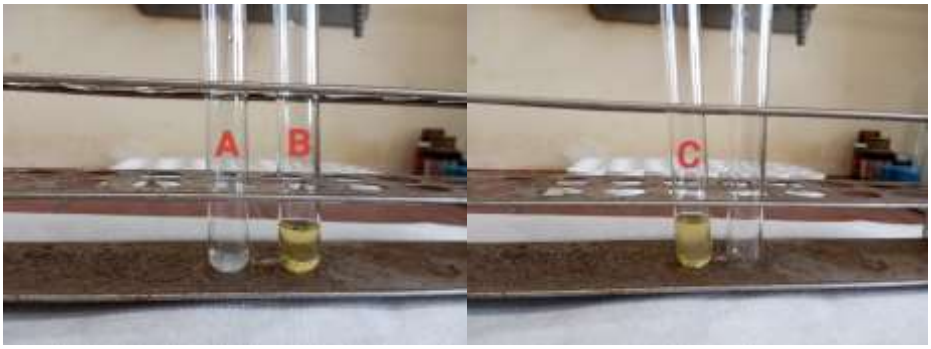

Figure S4. A) Non-irradiated reaction mixture, **B)** KI-glacial acetic acid solution, and **C)** resulting solution after mixture of **A** and **B** *(negative result)*.

Leaching Test of the Catalyst

In a glass vial containing GrF (1 mg), methanol (0.5 mL) was added, and then the suspension was sonicated for 30 min. Then, thioanisole (1 eq., 0.20 mmol, 25 mg) was added into the suspension and the reaction mixture was left stirring under blue LED irradiation (Kessil PR160L, 456 nm) for 2 h. Afterward, the solid was removed from the reaction mixture via filtration (pore size of filter 50 nm), and the conversion of the photooxidation was calculated (23%) by NMR. Then, the filtrate was allowed to proceed for an additional 16 h under irradiation, and the conversion was also calculated by NMR (23%).

1,3-Diphenylisobenzofuran (DPIBF) as A Selective Probe for Singlet Oxygen

FG dispersions (6 mg FG/3 mL solvent) in methanol (MeOH) or acetonitrile (MeCN) were placed in 1 cm magnetically stirred fluorescence cuvettes and contained the same amount of DPIBF from a stock solution. The samples were irradiated with a 470-nm LED array light source (Thorlabs; LED Array Light Sources; November 11th) at an intensity of 4.0 mW/cm² and a total output power of 253 mW, from a distance of 1.0 cm. MeOH and MeCN were HPLC gradient grade (99.9%; Fisher Scientific).

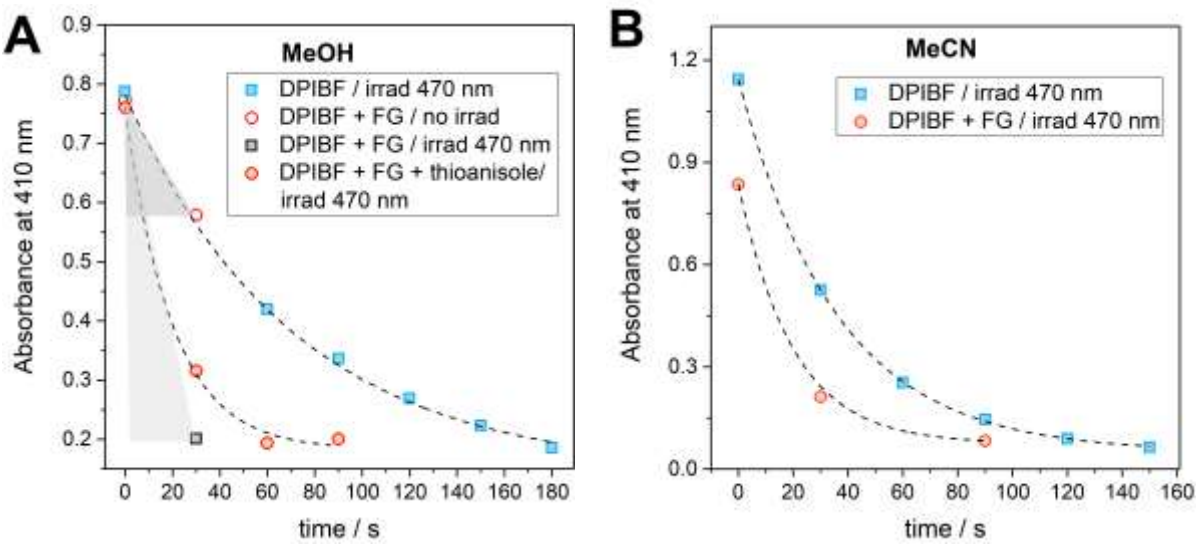

Figure S5. A) Degradation kinetics of DPIBF in MeOH under different conditions, monitored as the decrease in absorbance at the DPIBF absorption maximum. **B)** Photodegradation of DPIBF in MeCN in the presence and absence of FG under 470 nm light irradiation.

Although DPIBF is a selective singlet oxygen scavenger via usual [4+2] cycloaddition (forming the 2,5-endoperoxide that subsequently decomposes to *o*-dibenzoylbenzene), it can also undergo low-temperature auto-oxidation/self-sensitized photodegradation.[7] However, its rapid disappearance in MeOH under 470 nm irradiation of the FG dispersion, compared with the self-degradation kinetics, strongly indicates photodegradation by singlet oxygen (Figure S4A). As shown in Figure S5A, the entire amount of DPIBF (i.e., the 410-nm absorbance decreasing to the baseline) vanishes in MeOH within the first 30 seconds, whereas its FG-

sensitized photooxidation by singlet oxygen in MeCN is clearly less effective and closely follows its self-degradation curve in this solvent (Figure S5B).

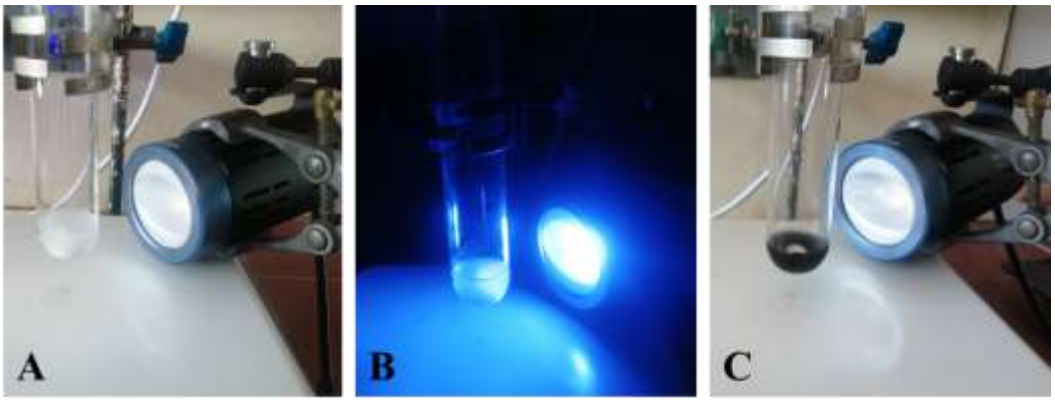

Figure S6. Setup utilized for the photochemical aerobic oxidation reaction (Blue LED, Kessil PR 160L, 456 nm). Reaction mixture before irradiation (A), during irradiation (B) and after completion of the reaction (C).

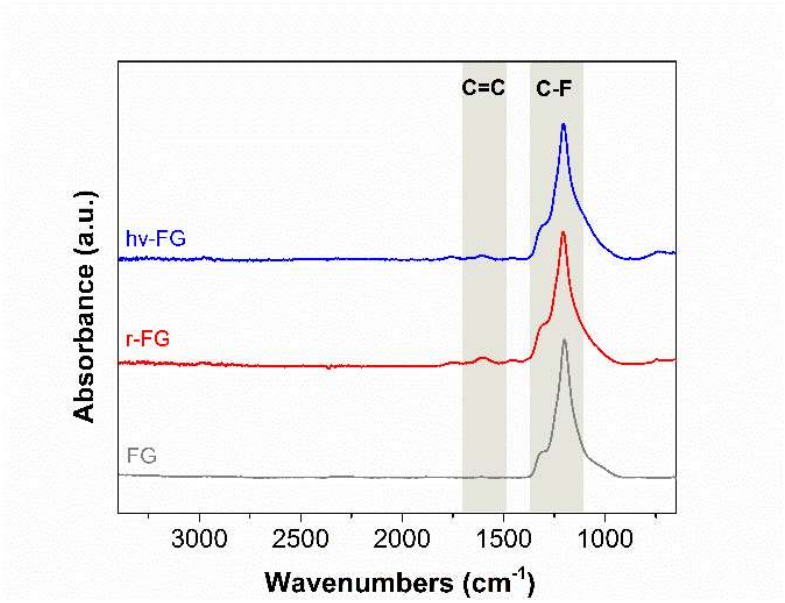

Figure S7. FTIR spectra of exfoliated FG by MeOH (FG), recovered FG after the first cycle (r-FG), and irradiated FG by LED 456 nm (hv-FG).

Computational Analysis

Computational details

The structures and the electronic transitions of pristine and defected fluorographene (FG) were explored by applying (time-dependent) density functional theory [(TD)DFT]. The finite-size models of FG were derived from perfluoroovalene (Figure S8), which was shown to represent the semi-local reactivity and optical properties of FG well.[8,9] For geometry optimizations, the CAM-B3LYP functional[10] including with the Grimme's empirical dispersion with Becke-Johnson damping (D3BJ)[11] was used, in combination with the def2-SVP basis set. For the analysis of electronic transitions, the same functional with the def2-TZVPP basis set was applied.[12,13] The bulk solvent effects were included via the implicit solvent model based on density (SMD)[14] with its Linear-Response variant[15,16] for the excited states. For selected models, an explicit solvent molecule (MeOH or MeCN) was added to enable analysis of solute-solvent charge transfer transitions. All calculations for finite-size models were performed with Gaussian16 program,[17] revision C.02.

The periodic model calculations were performed using the projector-augmented wave method implemented in the Vienna ab-initio simulation package (VASP) suite.[18,19] The potentials used in the present work were the latest GW potentials distributed with VASP (vasp.6.3). The supercell approach was used to model FG containing 1F defects (fluorine vacancies); we adopted the 3×3 supercell and modelled the radical defect by removing single fluorine atom (1F-) or three neighbouring F atoms (3F-), followed by relaxation of atomic positions. The energy cut-off for the plane-wave expansion was set to 400 eV, and the 3×3×1 *k*-point grid was used to sample the Brillouin zone of the supercell. The geometry of the radical defect and of the physisorbed methanol was attained by using the optimized van der Waals DFT functional optB86b-vdW.[20] The periodically repeated sheets were separated by at least 8 Å of vacuum. The differential charge densities were plotted using the VESTA suite.[21] The GW calculation was performed on top of the Kohn-Sham orbitals. The Green's function was iterated self-consistently including non-diagonal components of the self-energy (this method is denoted as qpGW$_0$). In GW calculation, we kept the 3×3×1 *k*-point grid (corresponding to the 9×9×1 *k*-point grid in the unit cell) and the energy cutoff of 400 eV. We added a large number of empty bands so GW calculations were performed using at least 1500 unoccupied bands, which is essential for their convergence.[22] The Bethe-Salpeter equation was solved on top of the GW$_0$ calculation using the same set of computational parameters.

For the interaction with MeOH, we modelled the radical defect by removing single fluorine atom (1F-) or three neighbouring F atoms (3F-) followed by relaxation of atomic positions. Then, we put a methanol molecule in the vicinity of the defect and relaxed the whole geometry (from several starting positions of the molecule). The optical spectrum was then calculated for the most favourable configuration. We used mainly TDDFT calculation in connection with the 4×4 supercell of FG. For the TDDFT was used dielectric-dependent range-separated hybrid functional (DDH).[23] The screening parameter was set to 1.6 and the fraction of exact exchange in the long-range was 0.25 (same as in the PBE0 functional).

PBC results

The test comparison for FG(-1F) on small 3×3 supercell showed that TDDFT@DDH provided both the FG optical bandgap of 5.97 eV and the S_1 excitation state of 3.83 eV in qualitative agreement with much more demanding BSE/GW_0 method (5.71 eV and 3.58 eV), which allowed to use the TDDFT@DDH for larger (and more realistic) 4×4 supercell.

For MeOH interacting with a single F-vacancy (denoted FG(-1F)-MeOH), periodic TDDFT@DDH calculation yielded a strong CT excitation at 2.8 eV using smaller 3×3 supercell and 3.0 eV with larger 4×4 supercell (Fig. S12). In the case of a 3F-vacancy, an analogous CT excitation was obtained from TDDFT@DDH with the VEE of 2.8 and 2.9 eV for the 3×3 and 4×4 supercell, respectively (Fig. S13).

Finite-size models of fluorographene (FG)

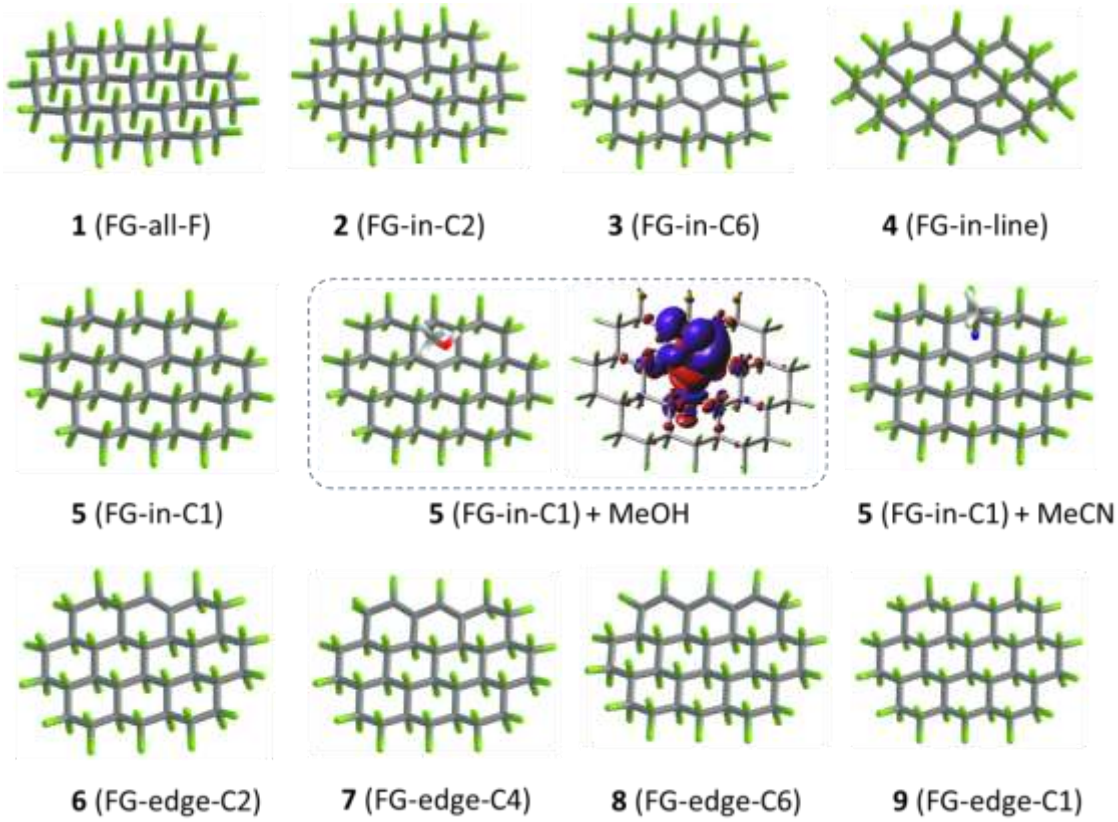

Figure S8. Finite-size models **1-9** of FG based on perfluoroovalene (**1**) optimized at the CAM-B3LYP-D3BJ/def2-SVP/SMD level of theory. For a 1F-vacancy structure **5** with an explicit MeOH molecule, an EDD plot (isovalue = 0.002e) for the $S_0 \rightarrow S_1$ transition showing increase (red) and decrease (blue) of the electron density upon the excitation is displayed.

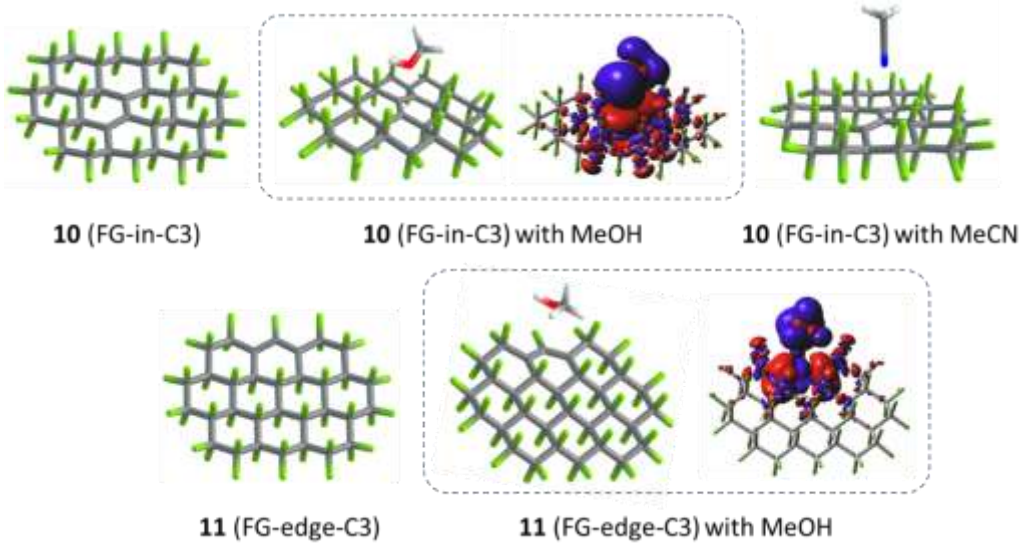

Figure S9. Finite-size models of 3F-vacancies in FG optimized at the CAM-B3LYP-D3BJ/def2-SVP/SMD level of theory. EDD plots (isovalue = 0.001e) for models including an explicit MeOH molecule showing increase (red) and decrease (blue) of the electron density upon the $S_0 \rightarrow S_1$ excitation are displayed.

Analysis of electronic transitions

Table S7 Multiplicity (*M*), vertical excitation energy (VEE) for the $S_0 \rightarrow S_1$ transition (in eV and nm), the oscillator strength (*f* in a.u.), and energies of frontier molecular orbitals (in eV) o at the CAM-B3LYP-D3BJ/def2-TZVPP/SMD level of theory for the structures optimized using the def2-SVP basis set.

No.	Description	*M*	VEE [eV]	VEE [nm]	f	HOMO [eV]	LUMO [eV]	H-L gap [eV]
1	perfluoroovalene, PFO (FG-all-F)	1	6.98	177	0.13	-11.11	-1.32	9.80
2	PFO-C2-defect (FG-in-C2)	1	5.88	211	0.00	-11.04	-2.36	8.68
3	PFO-C6-defect (FG-in-C6)	1	4.90	253	0.00	-10.65	-2.12	8.54
4	PFO-line-defect (FG-line)	1	3.83	324	1.16	-8.91	-2.85	6.07
5	PFO-(1C) radical (FG-in-C1)	2	4.04	307	0.00	-11.09	-3.98	7.10
5 + MeOH	PFO-(1C) radical (FG-in-C1) with MeOH	2	2.88	431	0.04	-9.56	-3.53	6.03
5 + MeCN	PFO-(1C) radical (FG-in-C1) with MeCN	2	4.44	279	0.00	-10.29	-3.40	6.89
6	PFO-edge-C2-defect (FG-edge-C2)	1	6.48	191	0.40	-10.87	-1.49	9.38
7	PFO-edge-C4-defect (FG-edge-C4)	1	5.14	241	0.73	-9.81	-2.01	7.79
8	PFO-edge-C6-defect (FG-edge-C6)	1	4.31	288	0.91	-8.72	-2.08	6.64
9	PFO-edge-C1-defect (FG-edge-C1)	2	4.97	249	0.00	-9.75	-2.72	7.03
10	PFO-(3C) radical defect (FG-in-C3)	2	3.51	353	0.01	-9.95	-4.03	5.92
10 + MeOH	PFO-(3C) radical defect (FG-in-C3) with MeOH	2	2.86	434	0.03	-9.31	-3.91	5.40
10 + MeCN	PFO-(3C) radical defect (FG-in-C3) with MeCN	2	3.45	360	0.01	-9.75	-3.86	5.89
11	PFO-(3C) edge radical defect (FG-edge-C3)	2	3.08	402	0.08	-9.75	-3.85	5.89
11 + MeOH	PFO-(3C) edge radical defect (FG-edge-C3)	2	2.71	458	0.04	-9.43	-3.78	5.66
MeOH	Methanol	1	7.61	163	0.00	-9.44	2.27	11.71
MeCN	Acetonitrile	1	7.88	157	0.00	-10.91	2.17	13.08

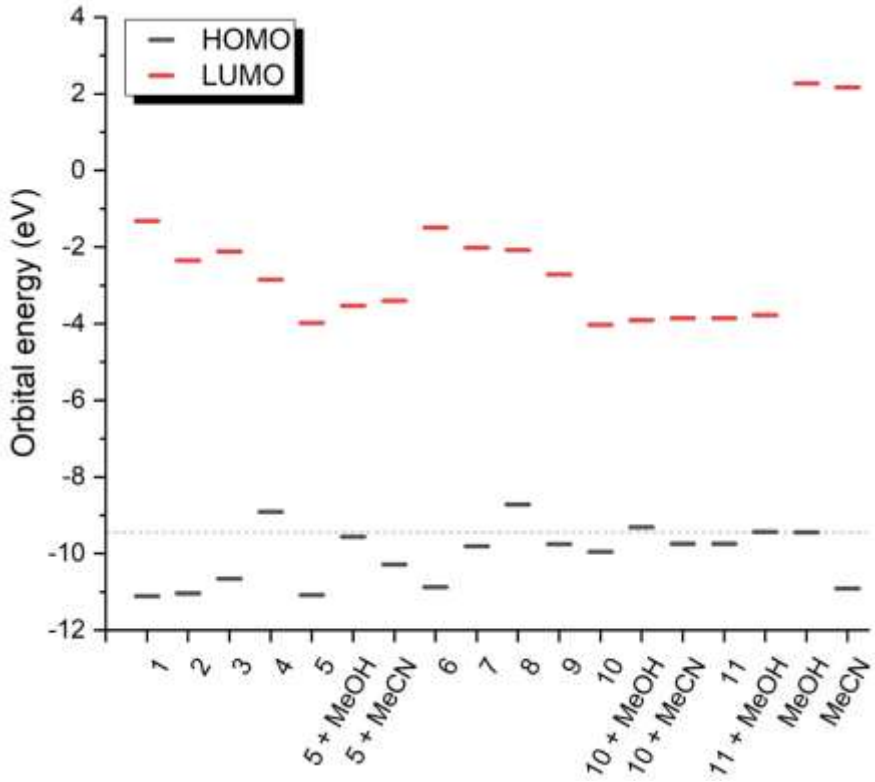

Figure S10. HOMO and LUMO energies (in eV) of finite-size models of FG displayed in Figures S7 and S8 calculated at the CAM-B3LYP-D3BJ/def2-TZVPP/SMD level of theory.

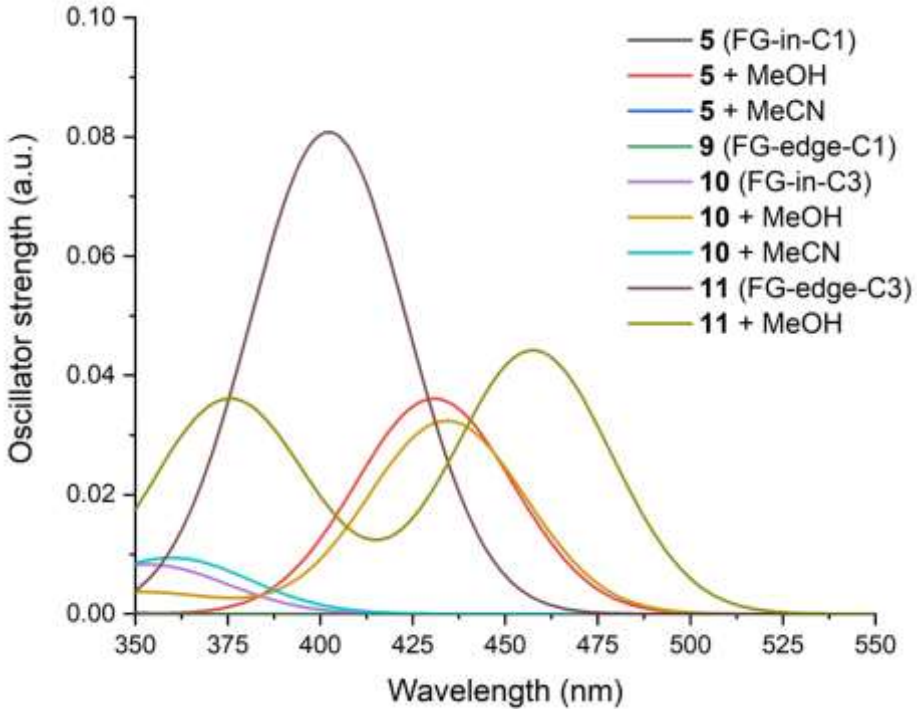

Figure S11. Absorption spectra of finite-size models of FG containing radical defects (1F- and 3F-vacancies) displayed in Figures S7 and S8 simulated at the LR-TD-CAM-B3LYP-D3BJ/def2-TZVPP/SMD level of theory (FWHM = 50 nm). Note that **5** and **5** + MeCN do not absorb in the shown spectral region.

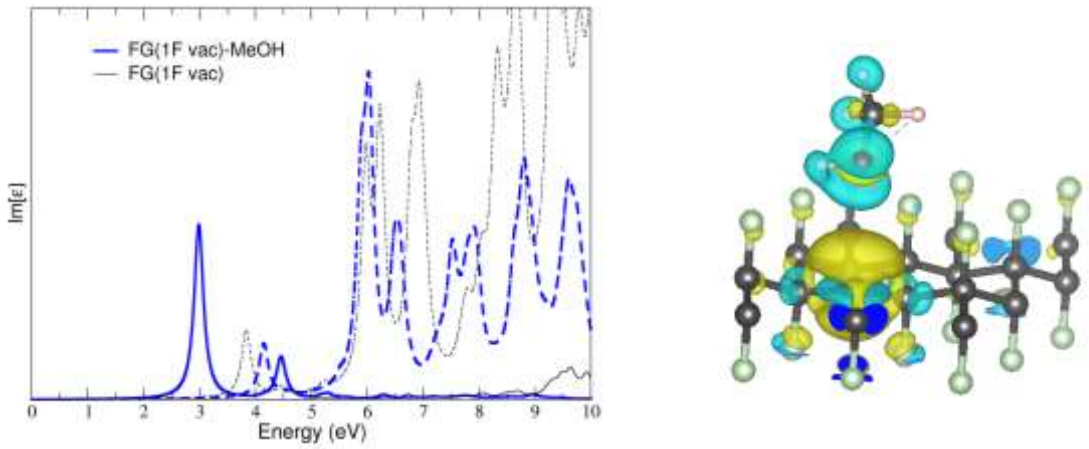

Figure S12. **Left:** Imaginary part of the dielectric function (proportional to absorption) for a periodic model of FG containing a 1F- radical defect w/o the methanol molecule in the vicinity of the defect. The full line corresponds to ε_{zz} (out-of-plane direction), dashed lines to ε_{xx} (in-plane direction). **Right**: the charge density difference between the S_1 state and the ground-state for FG containing 1F- radical defect.

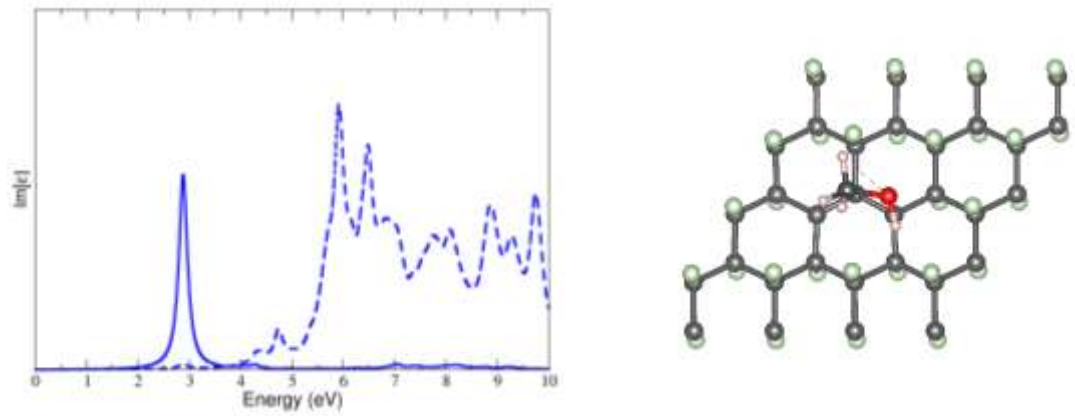

Figure S13. **Left:** Imaginary part of the dielectric function for periodic model of FG containing 3F- radical defect with the methanol molecule in the vicinity of the defect. The full line corresponds to ε_{zz} (out-of-plane direction), dashed lines to ε_{xx} (in-plane direction). **Right:** the relaxed geometry of FG(3F-)-MeOH.

Calculation of Production Rate, Environmental Factor (E), Reaction Mass Efficiency (RME) and Process Mass Intensity (PMI)

Calculation of Production Rate

Equation S1: Equation for calculation of production rate for heterogeneous catalysts.

$$Production\ Rate = \frac{product\ \mathbf{2a}\ (mmol)}{total\ catalyst\ amount\ (g)\ \times\ reaction\ time\ (h)}$$

Calculation of Environmental factor (E)

Equation S2: Equation for calculation of Environmental factor (E) for the applied protocols in the photochemical aerobic oxidation of sulfides.

$$E = \frac{mass\ of\ waste\ (mg) - isolated\ mass\ of\ product\ \mathbf{2a}\ (mg)}{isolated\ mass\ of\ product\ \mathbf{2a}\ (mg)}$$

Calculation of Reaction Mass Efficiency (RME)

Equation S3: Equation for calculation of Reaction Mass Efficiency (RME) for the applied protocols in the photochemical aerobic oxidation of sulfides.

$$RME = \frac{isolated\ mass\ of\ product\ \mathbf{2a}\ (mg)}{total\ mass\ of\ all\ chemical\ used\ (mg)}$$

Calculation of Process Mass Intensity (PMI)

Equation S4: Equation for calculation of Process Mass Intensity (PMI) for the applied protocols in the photochemical aerobic oxidation of sulfides.

$$PMI = \frac{1}{RME} = E + 1$$

Table S8

Catalyst	Productivity Rate (mmol g^{-1} h^{-1})	Environmental factor	RME	PMI
FG (our work)	11.1	15.4	0.061	16.4
[mpg-C_3N_4][24]	4.7	126.4	0.008	127.4
[CNO][25]	12.2	22.9	0.042	23.9
[C_3N_4 NSs-5h][26]	49.0	57.8	0.017	58.8
[BPCN][27]	9.3	122.1	0.008	123.1
[C_{60}/g-C_3N_4][28]	1.1	142.4	0.007	143.4
[SFCPDs][29]	98.6	47.4	0.021	48.4
[MWCNT-H_2TCPP][30]	5.7	444.1	0.002	445.1
[Pt1@oSWNT][31]	13.5	88.7	0.011	89.7
[SWNT-Ru][32]	12.3	96.4	0.010	97.4
[AQ-COF][33]	3.2	118.0	0.008	119.0
[$BiOBr_{(001)}$][34]	6.0	23.7	0.040	24.7
[LED 370 nm][35]	-	28.3	0.034	29.3

References

1 A. Bakandritsos, M. Pykal, P. Błoński, P. Jakubec, D. D. Chronopoulos, K. Poláková, V. Georgakilas, K. Čépe, O. Tomanec, V. Ranc, A. B. Bourlinos, R. Zbořil and M. Otyepka, *ACS Nano*, 2017, **11**, 2982–2991.
2 E. Skolia, P. L. Gkizis, N. F. Nikitas and C. G. Kokotos, *Green Chem.*, 2022, **24**, 4108–4118.
3 A. M. Thomas, D. R. Sherin, S. Asha, T. K. Manojkumar and G. Anilkumar, *Polyhedron*, 2020, **176**, 114269.
4 T. Delcaillau, A. Bismuto, Z. Lian and B. Morandi, *Angew. Chem. Int. Ed.*, 2020, **59**, 2110–2114.
5 D. C. Lenstra, V. Vedovato, E. Ferrer Flegeau, J. Maydom and M. C. Willis, *Org. Lett.*, 2016, **18**, 2086–2089.
6 H.-L. Yue and M. Klussmann, *Synlett*, 2016, **27**, 2505–2509.
7 J. A. Howard and G. D. Mendenhall, *Can. J. Chem.*, 1975, **53**, 2199–2201.
8 M. Medveď, G. Zoppellaro, J. Ugolotti, D. Matochová, P. Lazar, T. Pospíšil, A. Bakandritsos, J. Tuček, R. Zbořil and M. Otyepka, *Nanoscale*, 2018, **10**, 4696–4707.
9 G. Zoppellaro, M. Medveď, V. Hrubý, R. Zbořil, M. Otyepka and P. Lazar, *J. Am. Chem. Soc.*, 2024, **146**, 15010–15018.
10 T. Yanai, D. P. Tew and N. C. Handy, *Chem. Phys. Lett.*, 2004, **393**, 51–57.
11 S. Grimme, S. Ehrlich and L. Goerigk, *J. Comput. Chem.*, 2011, **32**, 1456–1465.
12 F. Weigend and R. Ahlrichs, *Phys. Chem. Chem. Phys.*, 2005, **7**, 3297–3305.
13 F. Weigend, *Phys. Chem. Chem. Phys.*, 2006, **8**, 1057–1065.
14 A. V. Marenich, C. J. Cramer and D. G. Truhlar, *J. Phys. Chem. B*, 2009, **113**, 6378–6396.
15 M. Cossi and V. Barone, *J. Chem. Phys.*, 2001, **115**, 4708–4717.
16 R. Cammi and B. Mennucci, *J. Chem. Phys.*, 1999, **110**, 9877–9886.
17 M. J. Frisch, et al., Gaussian 16, Revision C.02 Gaussian, Inc., Wallingfort CT 2016.
18 P. E. Blöchl, *Phys. Rev. B*, 1994, **50**, 17953–17979.
19 G. Kresse and D. Joubert, *Phys. Rev. B*, 1999, **59**, 1758–1775.
20 J. Klimeš, D. R. Bowler and A. Michaelides, *Phys. Rev. B*, 2011, **83**, 195131.
21 K. Momma and F. Izumi, *J. Appl. Crystallogr.*, 2011, **44**, 1272–1276.
22 F. Karlický and M. Otyepka, *Ann. Phys.*, 2014, **526**, 408–414.
23 W. Chen, G. Miceli, G.-M. Rignanese and A. Pasquarello, *Phys. Rev. Mater.*, 2018, **2**, 073803.
24 P. Zhang, Y. Wang, H. Li and M. Antonietti, *Green Chem.*, 2012, **14**, 1904–1908.
25 H. Wang, S. Jiang, S. Chen, D. Li, X. Zhang, W. Shao, X. Sun, J. Xie, Z. Zhao, Q. Zhang, Y. Tian and Y. Xie, *Adv. Mater.*, 2016, **28**, 6940–6945.
26 J. Li, Y. Chen, X. Yang, S. Gao and R. Cao, *J. Catal.*, 2020, **381**, 579–589.
27 Z. Xie, W. Wang, X. Ke, X. Cai, X. Chen, S. Wang, W. Lin and X. Wang, *Appl. Catal. B Environ.*, 2023, **325**, 122312.
28 X. Chen, K. Deng, P. Zhou and Z. Zhang, *ChemSusChem*, 2018, **11**, 2444–2452.
29 Q. Song, W. Li, F. Shan, X. Peng, L. Wang, Z. Wang and X.-Q. Yu, *Nano Lett.*, 2024, **24**, 13895–13902.
30 S. Rayati, A. Zamanifard, F. Nejabat and S. Hoseini, *Mol. Catal.*, 2021, **516**, 111950.

31 D. González-Muñoz, J. Alemán, M. Blanco and S. Cabrera, *J. Catal.*, 2022, **413**, 274–283.
32 P. Blanco-Caamano, C. Navío, M. Blanco and J. Aleman, *J. Colloid Interface Sci.*, 2024, **669**, 495–505.
33 Q. Li, X. Lan, G. An, L. Ricardez-Sandoval, Z. Wang and G. Bai, *ACS Catal.*, 2020, **10**, 6664–6675.
34 H. Wang, S. Chen, D. Yong, X. Zhang, S. Li, W. Shao, X. Sun, B. Pan and Y. Xie, *J. Am. Chem. Soc.*, 2017, **139**, 4737–4742.
35 E. Skolia, P. L. Gkizis, N. F. Nikitas and C. G. Kokotos, *Green Chem.*, 2022, **24**, 4108–4118.

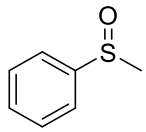
O
S

2a

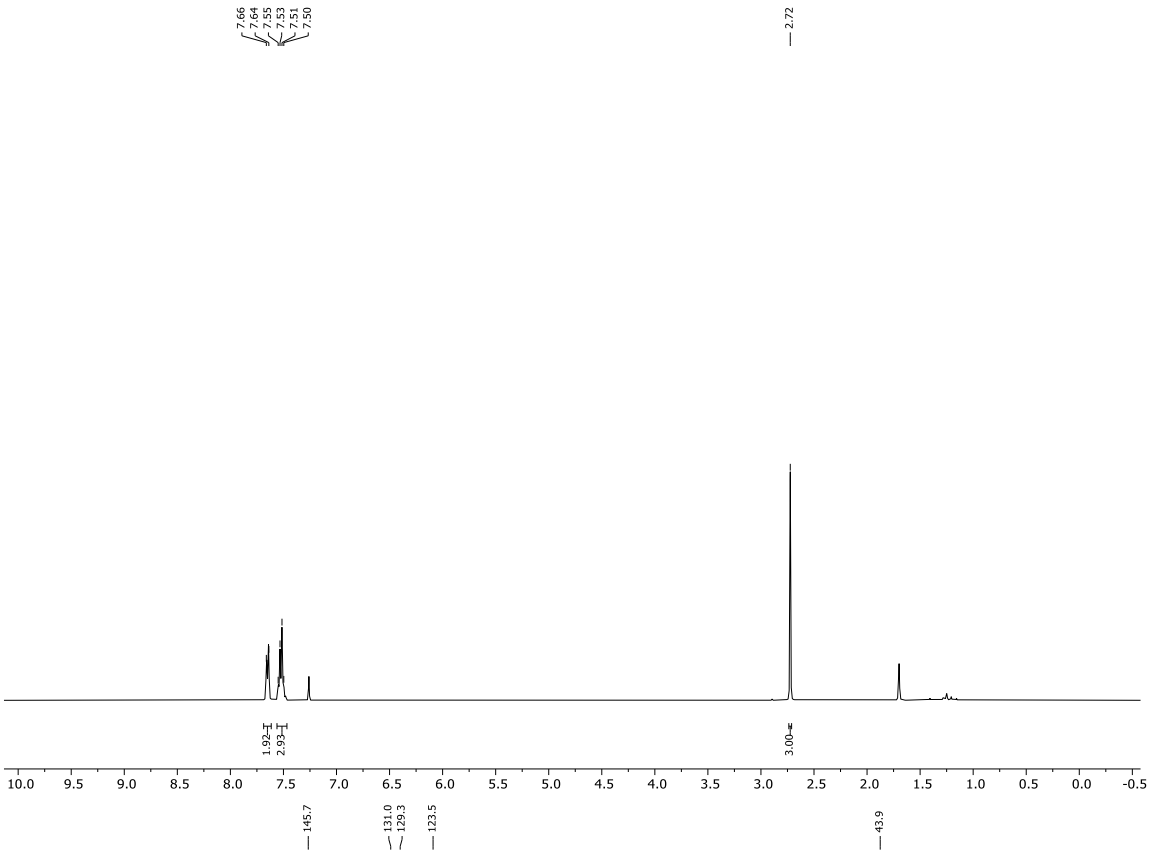
7.66
7.64
7.55
7.53
7.51
7.50
2.72
1.92
2.93
3.00
10.0 9.5 9.0 8.5 8.0 7.5 7.0 6.5 6.0 5.5 5.0 4.5 4.0 3.5 3.0 2.5 2.0 1.5 1.0 0.5 0.0 -0.5

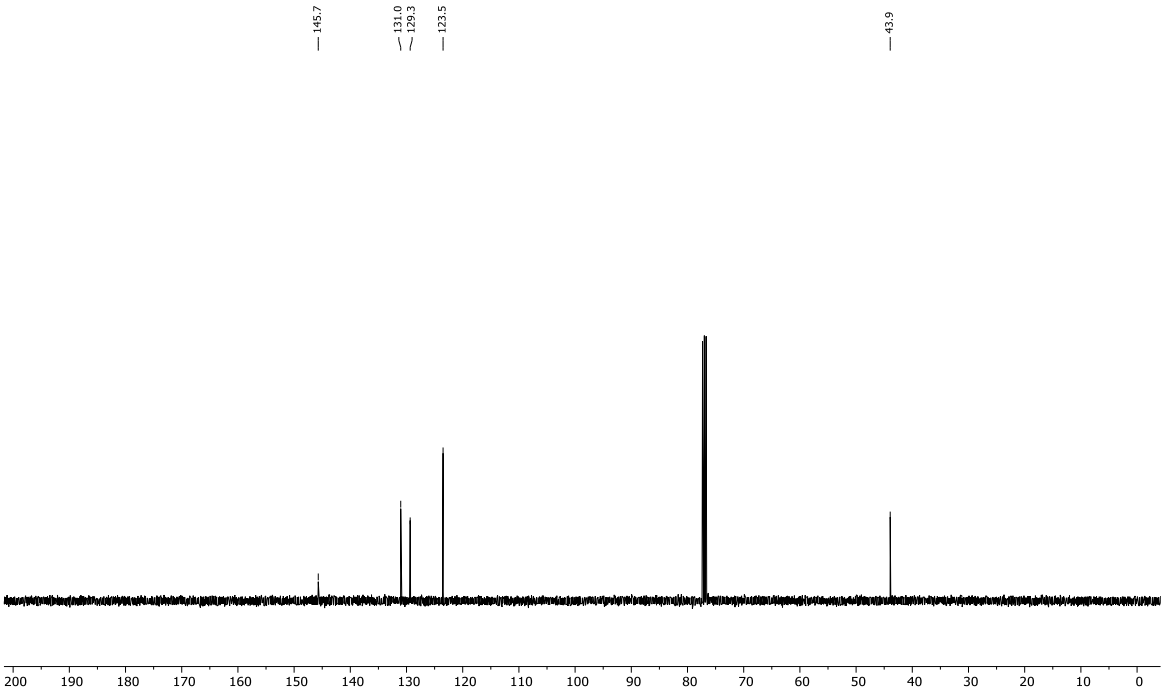
145.7
131.0
129.3
123.5
43.9
200 190 180 170 160 150 140 130 120 110 100 90 80 70 60 50 40 30 20 10 0

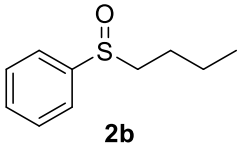

2b

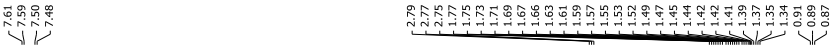
7.61
7.59
7.50
7.48
2.79
2.77
2.75
1.77
1.75
1.73
1.71
1.69
1.67
1.66
1.63
1.61
1.59
1.57
1.55
1.53
1.52
1.49
1.47
1.45
1.44
1.42
1.42
1.41
1.39
1.37
1.35
1.34
0.91
0.89
0.87

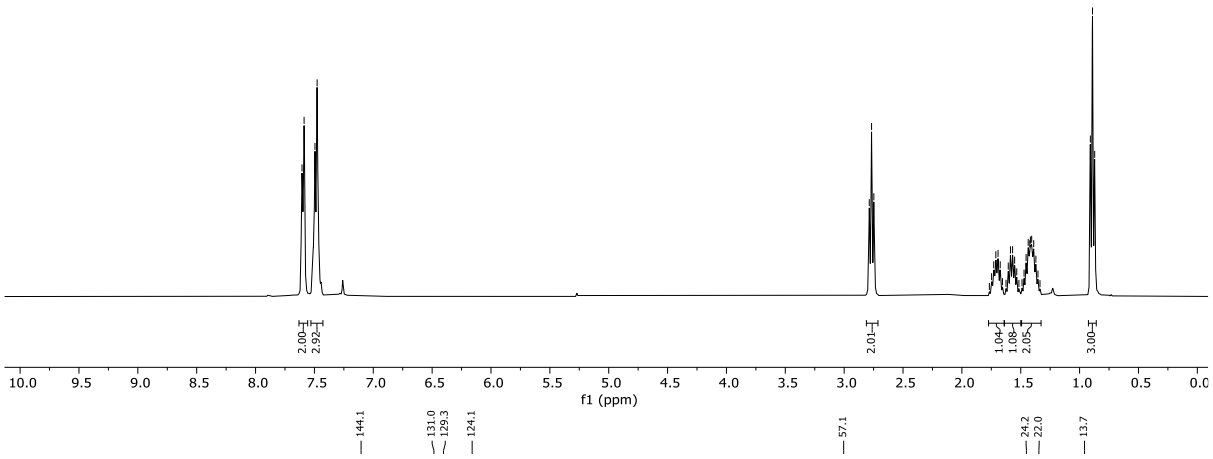
2.00
2.92
2.01
1.04
1.08
2.05
3.00
10.0 9.5 9.0 8.5 8.0 7.5 7.0 6.5 6.0 5.5 5.0 4.5 4.0 3.5 3.0 2.5 2.0 1.5 1.0 0.5 0.0
f1 (ppm)
144.1
131.0
129.3
124.1
57.1
24.2
22.0
13.7

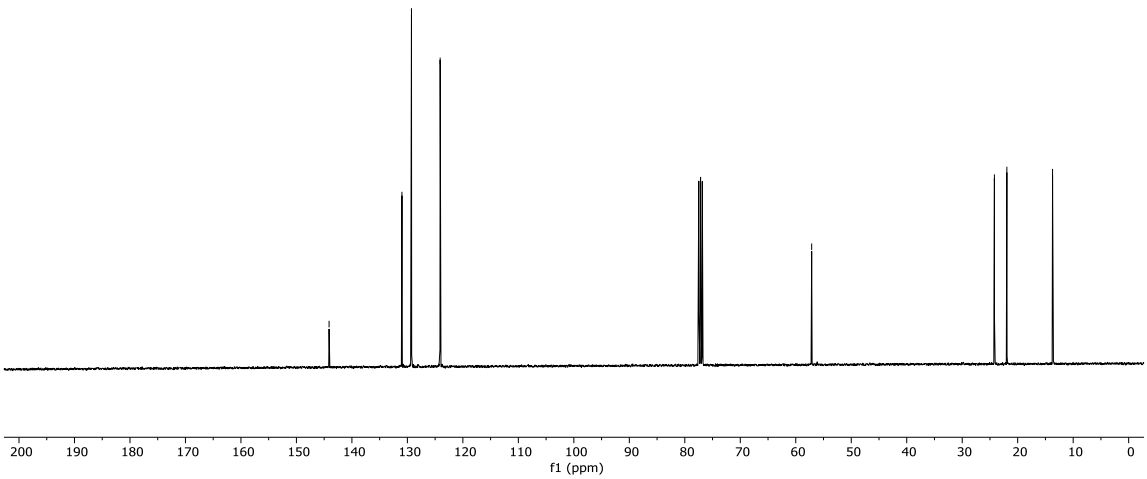
200 190 180 170 160 150 140 130 120 110 100 90 80 70 60 50 40 30 20 10 0
f1 (ppm)

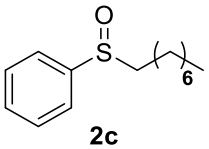
O
S
6

2c

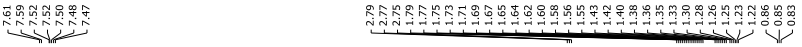
7.61
7.59
7.52
7.52
7.50
7.48
7.47
2.79
2.77
2.75
1.79
1.77
1.75
1.73
1.71
1.69
1.67
1.65
1.64
1.62
1.60
1.58
1.56
1.55
1.43
1.42
1.40
1.38
1.36
1.35
1.33
1.30
1.28
1.26
1.25
1.23
1.22
0.86
0.85
0.83

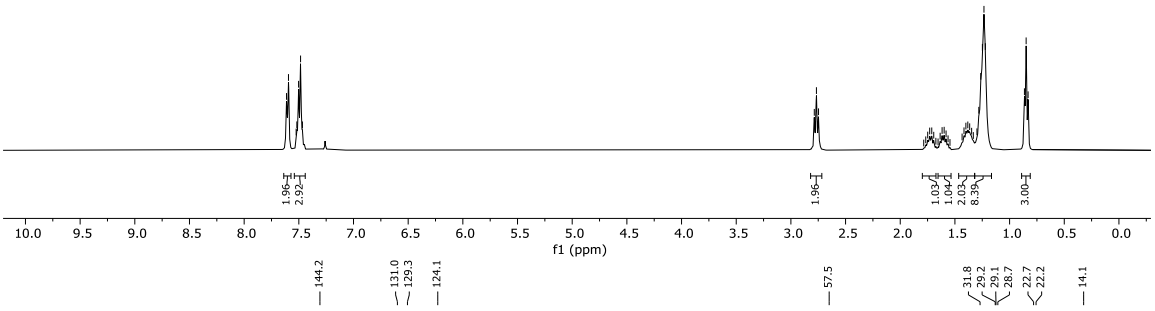
1.96
2.92
1.96
1.03
1.04
2.03
8.39
3.00
10.0
9.5
9.0
8.5
8.0
7.5
7.0
6.5
6.0
5.5
5.0
4.5
4.0
3.5
3.0
2.5
2.0
1.5
1.0
0.5
0.0
f1 (ppm)

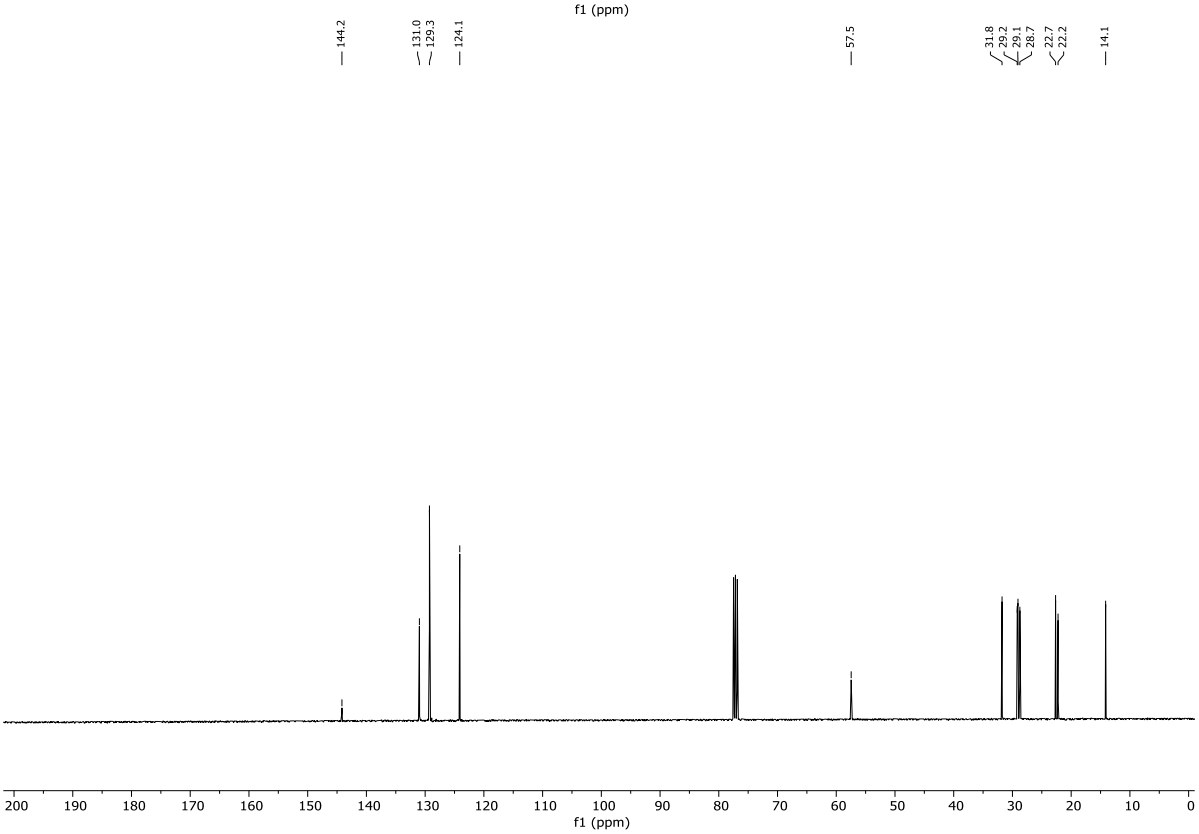
144.2
131.0
129.3
124.1
57.5
31.8
29.2
29.1
28.7
22.7
22.2
14.1
200
190
180
170
160
150
140
130
120
110
100
90
80
70
60
50
40
30
20
10
0
f1 (ppm)

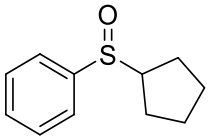

2d

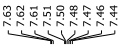
7.63
7.62
7.61
7.51
7.50
7.48
7.47
7.46
7.44


3.13
3.11
3.09
3.08
3.06
2.10
2.09
2.07
2.05
2.04
1.82
1.80
1.79
1.77
1.73
1.72
1.71
1.70
1.69
1.67
1.66
1.65
1.63
1.61
1.59
1.57
1.56

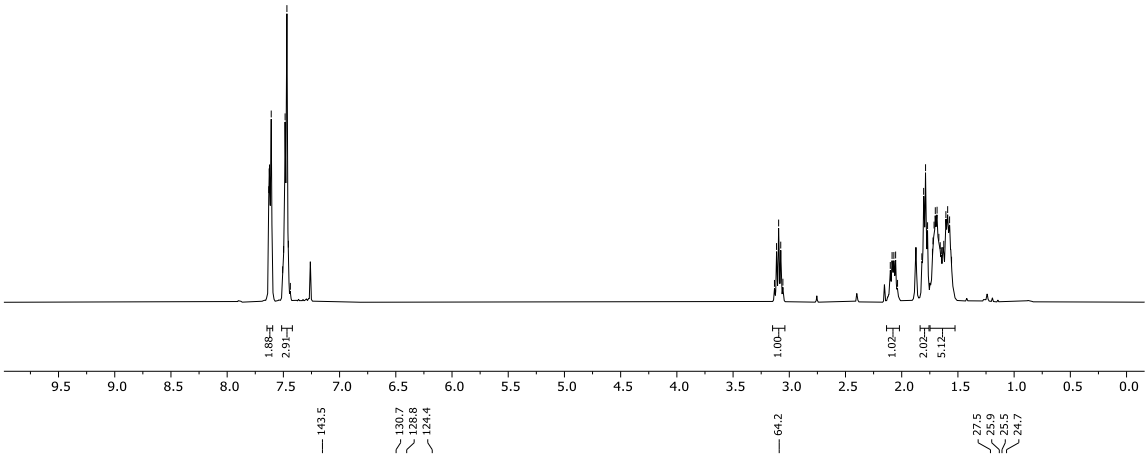
1.88
2.91
1.00
1.02
2.02
5.12
9.5
9.0
8.5
8.0
7.5
7.0
6.5
6.0
5.5
5.0
4.5
4.0
3.5
3.0
2.5
2.0
1.5
1.0
0.5
0.0

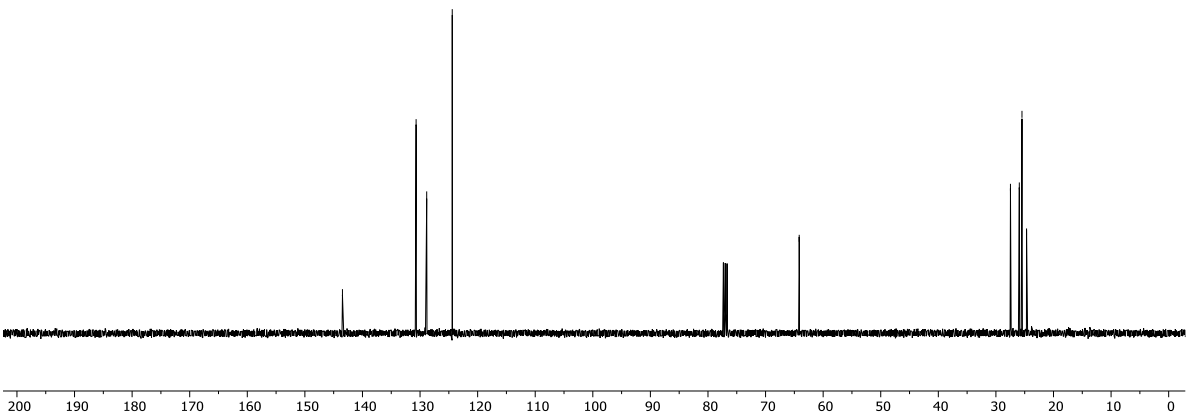
143.5
130.7
128.8
124.4
64.2
27.5
25.9
25.5
24.7
200
190
180
170
160
150
140
130
120
110
100
90
80
70
60
50
40
30
20
10
0

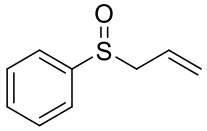
O
S

2e

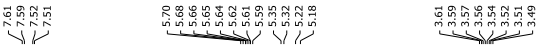
7.61
7.59
7.52
7.51
5.70
5.68
5.66
5.65
5.64
5.62
5.61
5.59
5.35
5.32
5.22
5.18
3.61
3.59
3.57
3.56
3.54
3.52
3.51
3.49

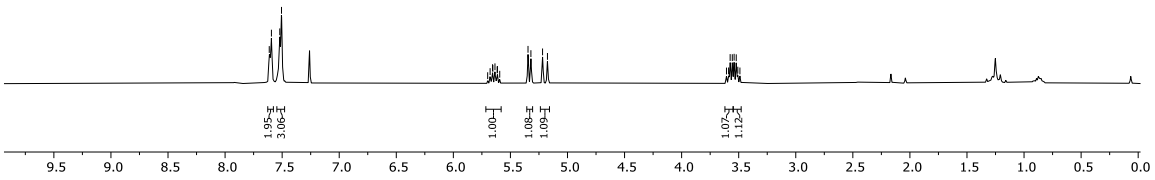
1.95
3.06
1.00
1.08
1.09
1.07
1.12
9.5
9.0
8.5
8.0
7.5
7.0
6.5
6.0
5.5
5.0
4.5
4.0
3.5
3.0
2.5
2.0
1.5
1.0
0.5
0.0

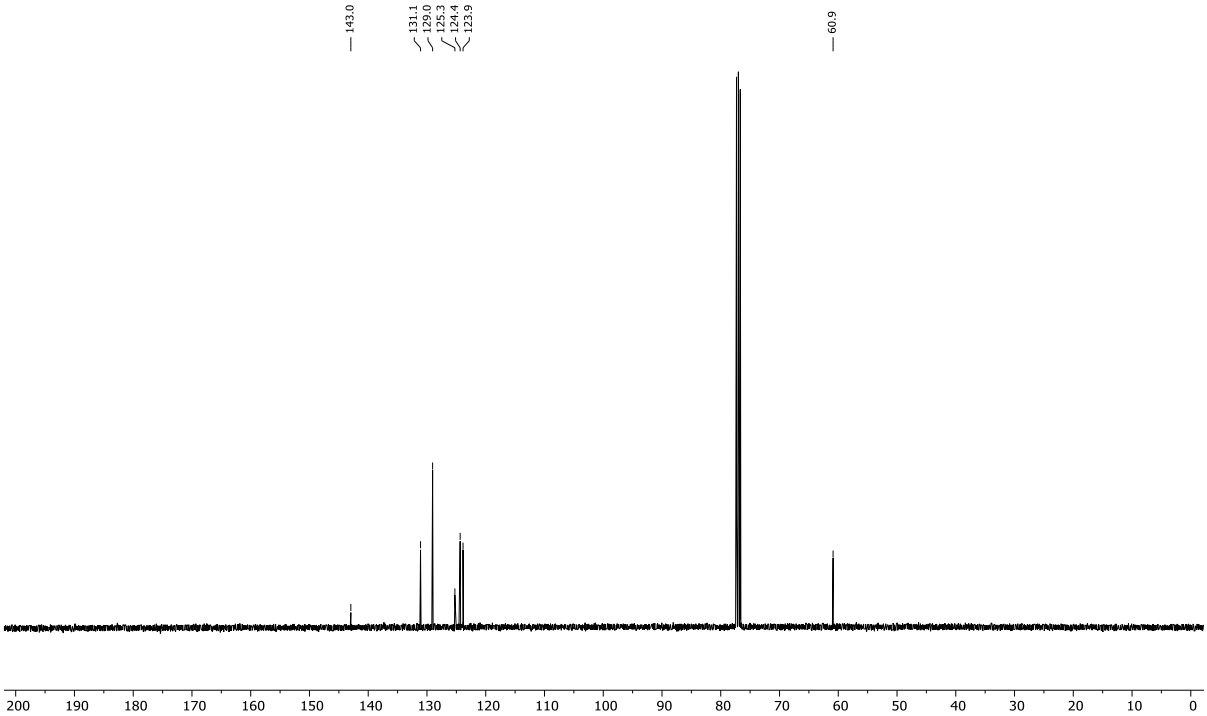
143.0
131.1
129.0
125.3
124.4
123.9
60.9
200
190
180
170
160
150
140
130
120
110
100
90
80
70
60
50
40
30
20
10
0

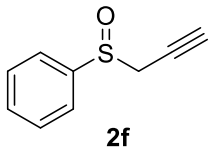

2f

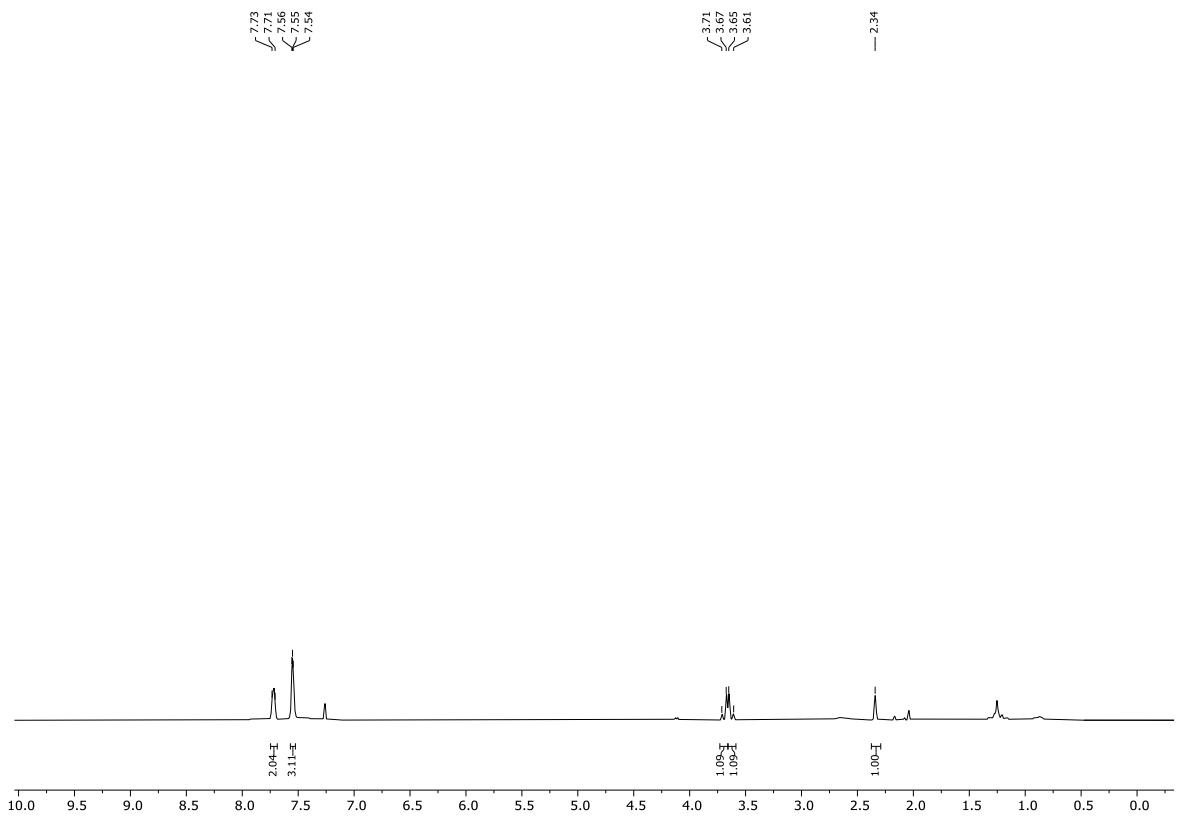
7.73
7.71
7.56
7.55
7.54
3.71
3.67
3.65
3.61
2.34
2.04
3.11
1.09
1.09
1.00
10.0 9.5 9.0 8.5 8.0 7.5 7.0 6.5 6.0 5.5 5.0 4.5 4.0 3.5 3.0 2.5 2.0 1.5 1.0 0.5 0.0

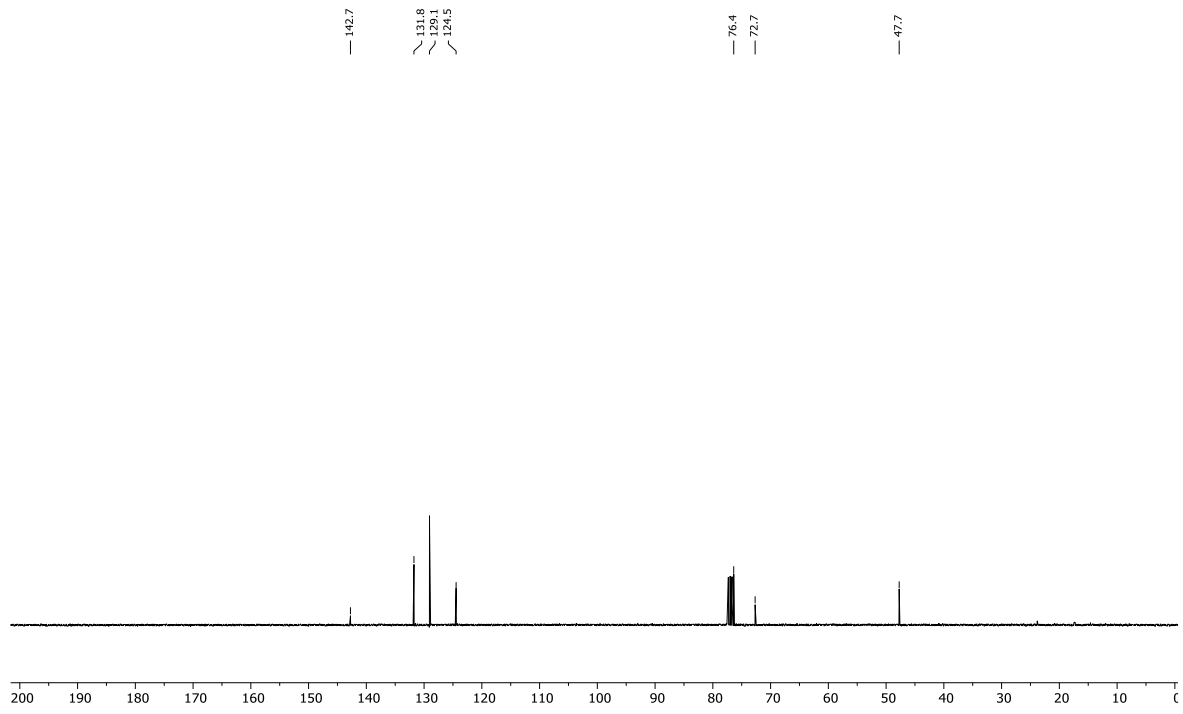
142.7
131.8
129.1
124.5
76.4
72.7
47.7
200 190 180 170 160 150 140 130 120 110 100 90 80 70 60 50 40 30 20 10

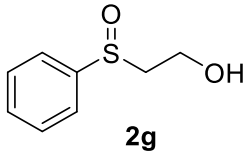
O
S
OH

2g

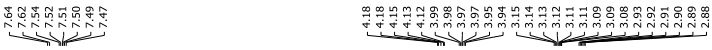
7.64
7.62
7.54
7.52
7.51
7.50
7.49
7.47
4.18
4.18
4.15
4.13
4.12
3.99
3.98
3.97
3.97
3.95
3.94
3.15
3.14
3.13
3.12
3.11
3.11
3.09
3.09
3.08
2.93
2.92
2.91
2.90
2.89
2.88

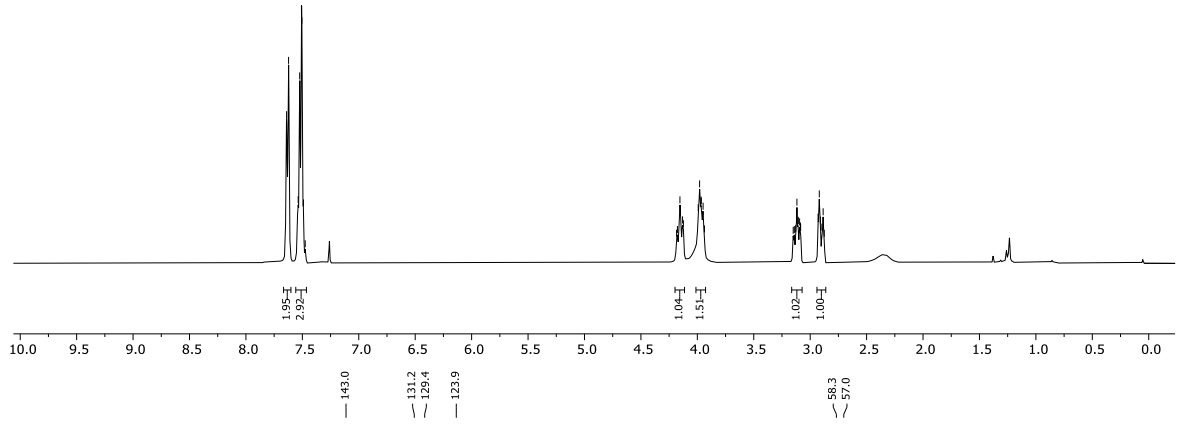
1.95
2.92
1.04
1.51
1.02
1.00
10.0
9.5
9.0
8.5
8.0
7.5
7.0
6.5
6.0
5.5
5.0
4.5
4.0
3.5
3.0
2.5
2.0
1.5
1.0
0.5
0.0

143.0
131.2
129.4
123.9
58.3
57.0

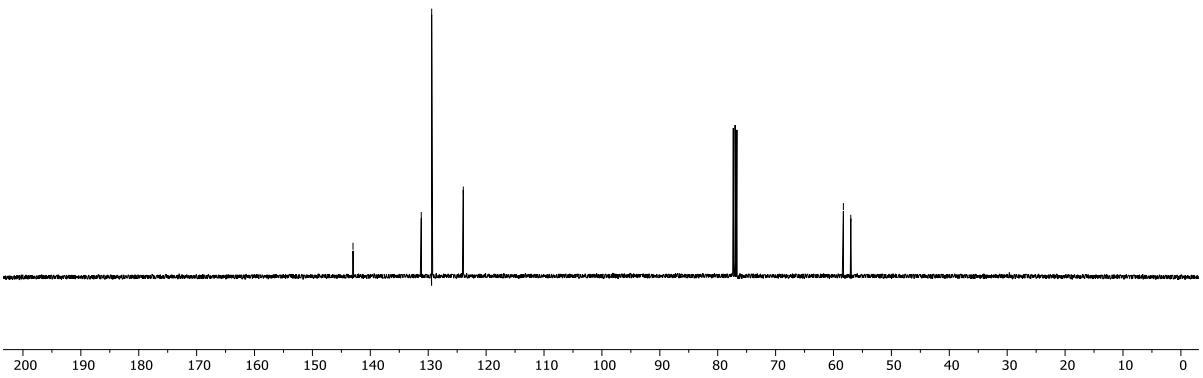
200
190
180
170
160
150
140
130
120
110
100
90
80
70
60
50
40
30
20
10
0

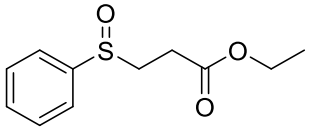

2h

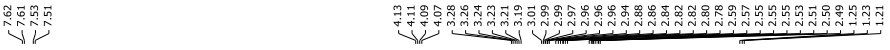
7.62
7.61
7.53
7.51
4.13
4.11
4.09
4.07
3.28
3.26
3.24
3.23
3.21
3.19
3.01
2.99
2.99
2.97
2.96
2.96
2.96
2.94
2.88
2.86
2.84
2.82
2.82
2.80
2.78
2.59
2.57
2.55
2.55
2.55
2.53
2.51
2.50
2.49
1.25
1.23
1.21

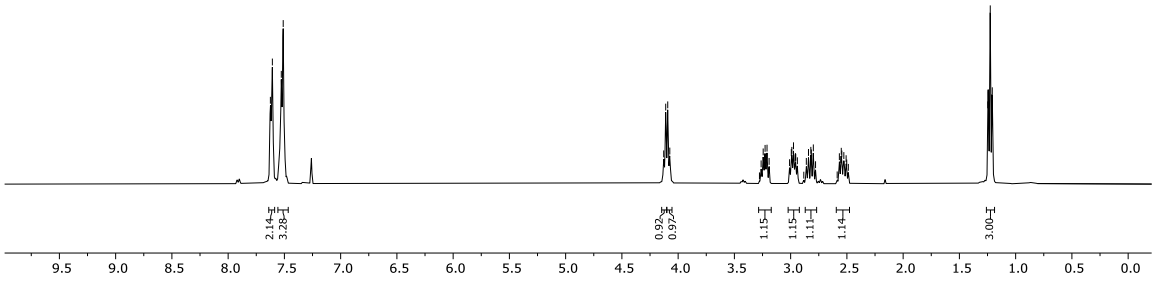
2.14
3.28
0.92
0.92
1.15
1.15
1.11
1.14
3.00
9.5 9.0 8.5 8.0 7.5 7.0 6.5 6.0 5.5 5.0 4.5 4.0 3.5 3.0 2.5 2.0 1.5 1.0 0.5 0.0

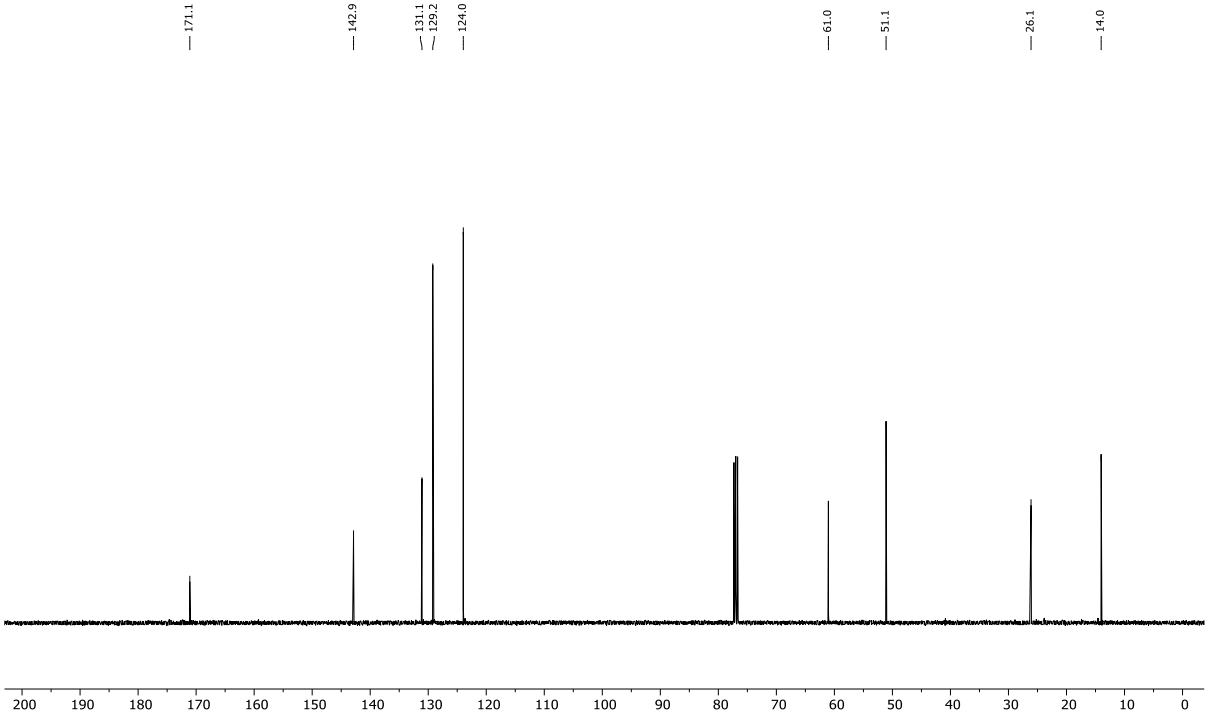
171.1
142.9
131.1
129.2
124.0
61.0
51.1
26.1
14.0
200 190 180 170 160 150 140 130 120 110 100 90 80 70 60 50 40 30 20 10 0

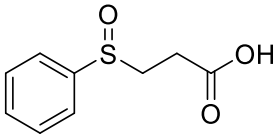
O
S
OH
O

2i

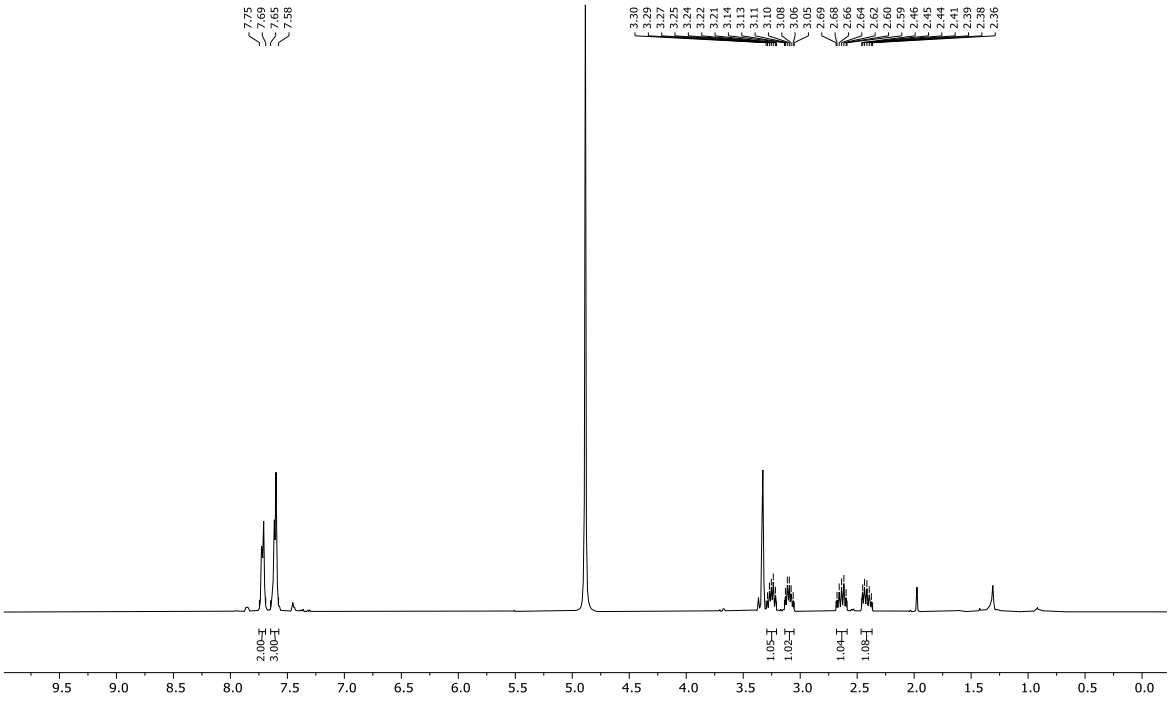
7.75
7.69
7.65
7.58
3.30
3.29
3.27
3.25
3.24
3.22
3.21
3.14
3.13
3.11
3.10
3.08
3.06
3.05
2.69
2.68
2.66
2.64
2.62
2.60
2.59
2.46
2.45
2.44
2.41
2.39
2.38
2.36
2.00
3.00
1.05
1.02
1.04
1.08
9.5
9.0
8.5
8.0
7.5
7.0
6.5
6.0
5.5
5.0
4.5
4.0
3.5
3.0
2.5
2.0
1.5
1.0
0.5
0.0

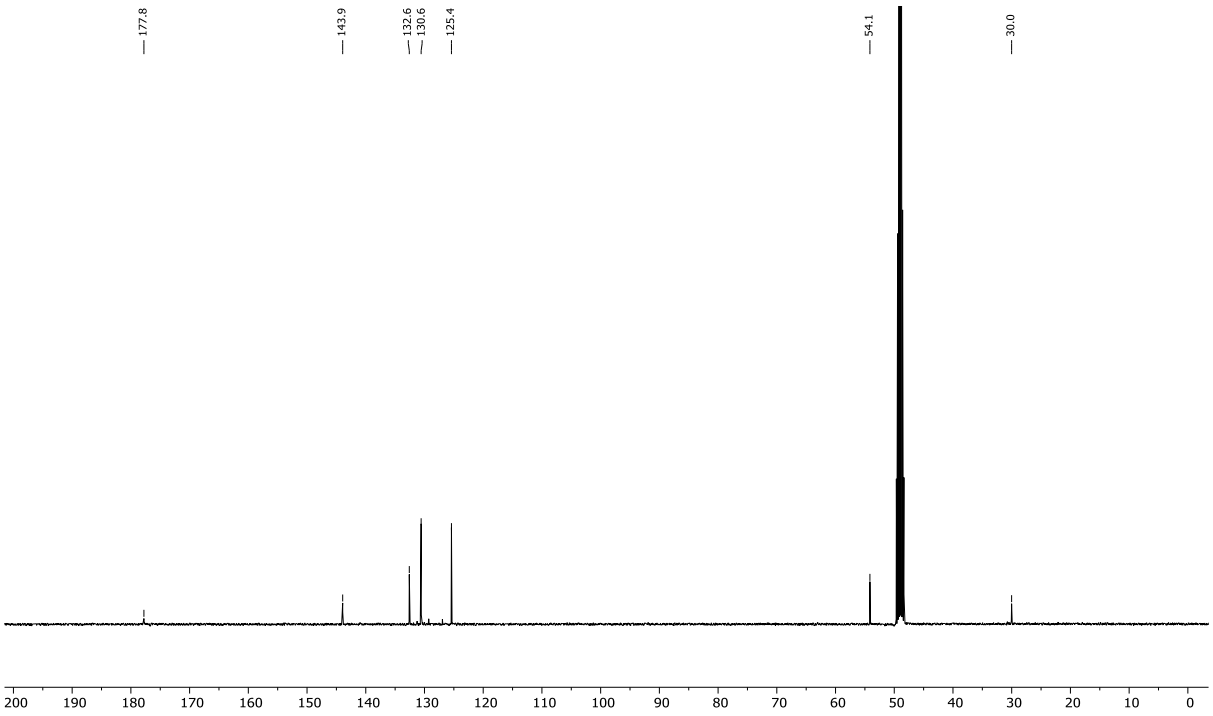
177.8
143.9
132.6
130.6
125.4
54.1
30.0
200
190
180
170
160
150
140
130
120
110
100
90
80
70
60
50
40
30
20
10
0

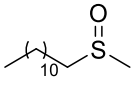
O
S
10

2j

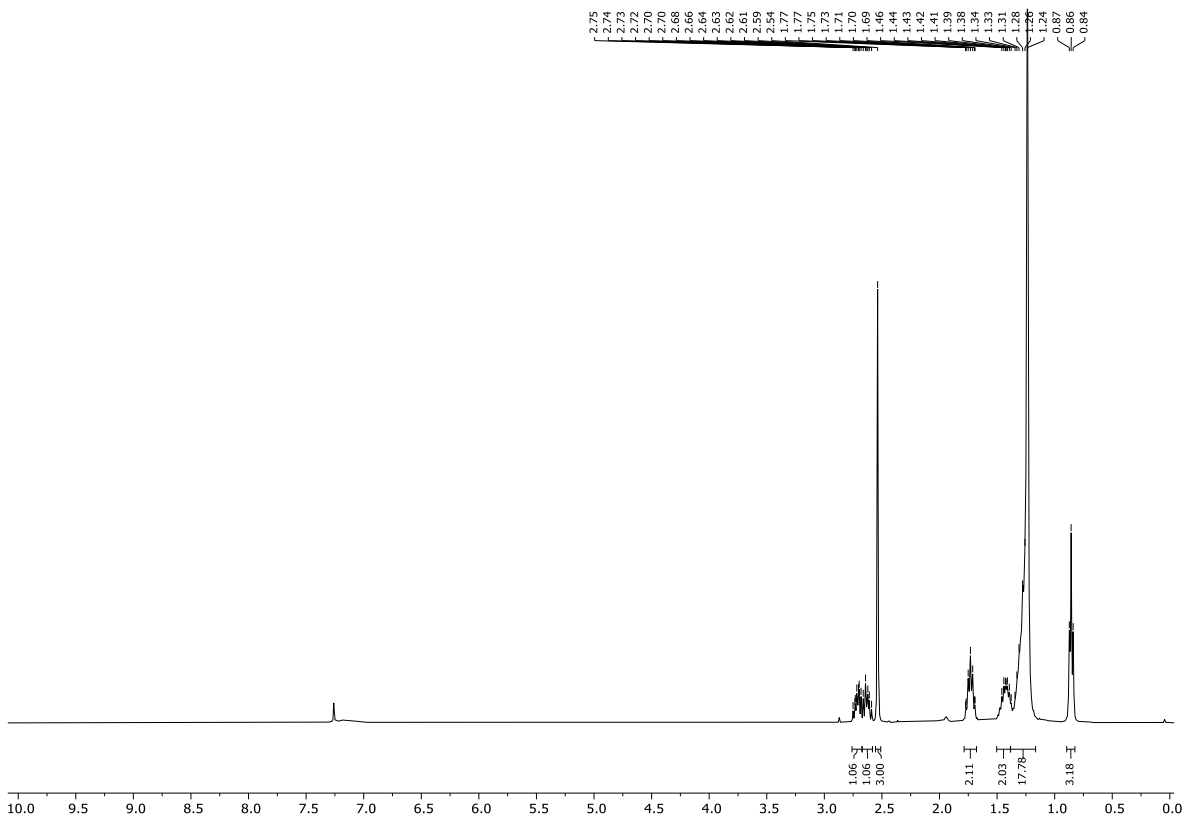
2.75
2.74
2.73
2.72
2.70
2.70
2.68
2.66
2.64
2.63
2.62
2.61
2.59
2.54
1.77
1.77
1.75
1.73
1.71
1.70
1.69
1.46
1.44
1.43
1.42
1.41
1.39
1.38
1.34
1.33
1.31
1.28
1.26
1.24
0.87
0.86
0.84
1.06
1.06
3.00
2.11
2.03
17.78
3.18
10.0
9.5
9.0
8.5
8.0
7.5
7.0
6.5
6.0
5.5
5.0
4.5
4.0
3.5
3.0
2.5
2.0
1.5
1.0
0.5
0.0

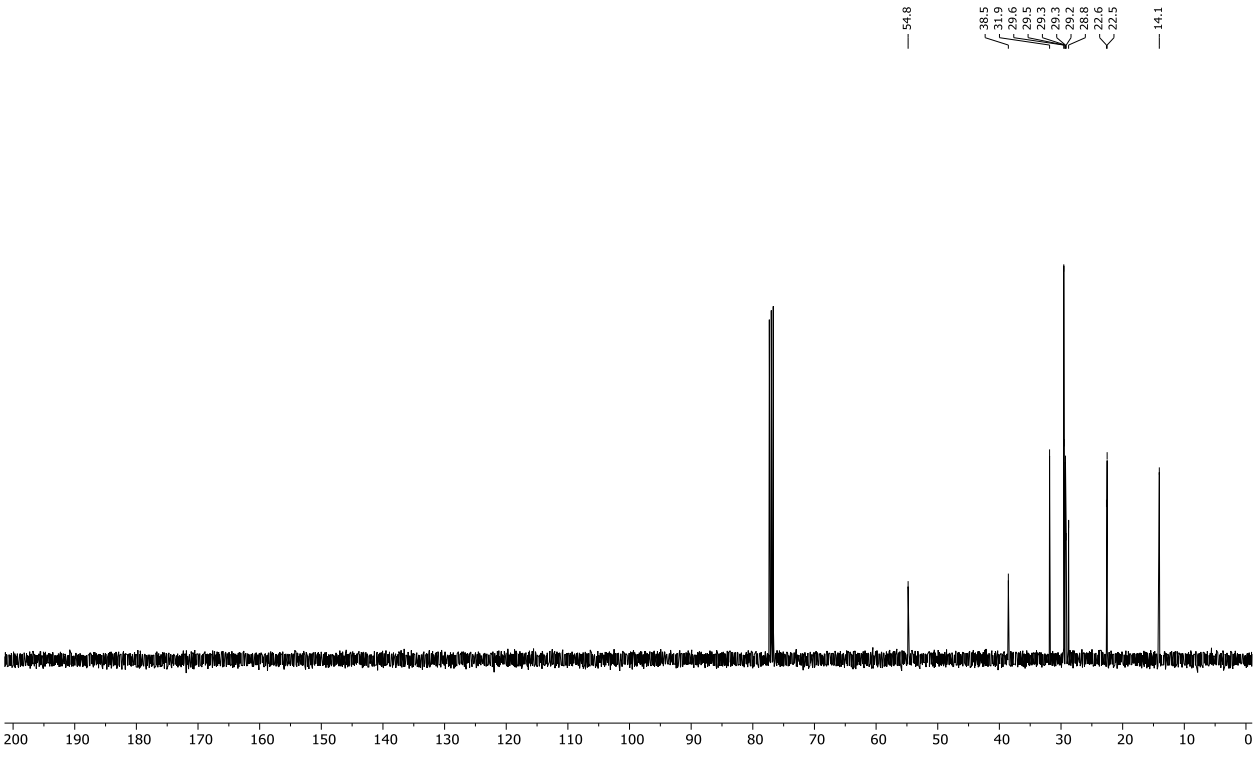
54.8
38.5
31.9
29.6
29.5
29.3
29.3
29.2
28.8
22.6
22.5
14.1
200
190
180
170
160
150
140
130
120
110
100
90
80
70
60
50
40
30
20
10
0

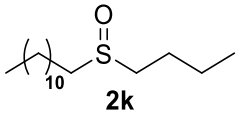
O
S
10

2k

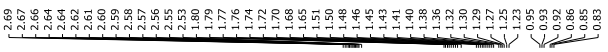
2.69
2.67
2.66
2.64
2.64
2.62
2.61
2.60
2.59
2.58
2.57
2.56
2.55
2.53
1.80
1.79
1.77
1.76
1.74
1.72
1.70
1.68
1.65
1.51
1.50
1.48
1.46
1.45
1.43
1.41
1.40
1.38
1.36
1.32
1.30
1.29
1.27
1.25
1.23
0.95
0.93
0.92
0.86
0.85
0.83

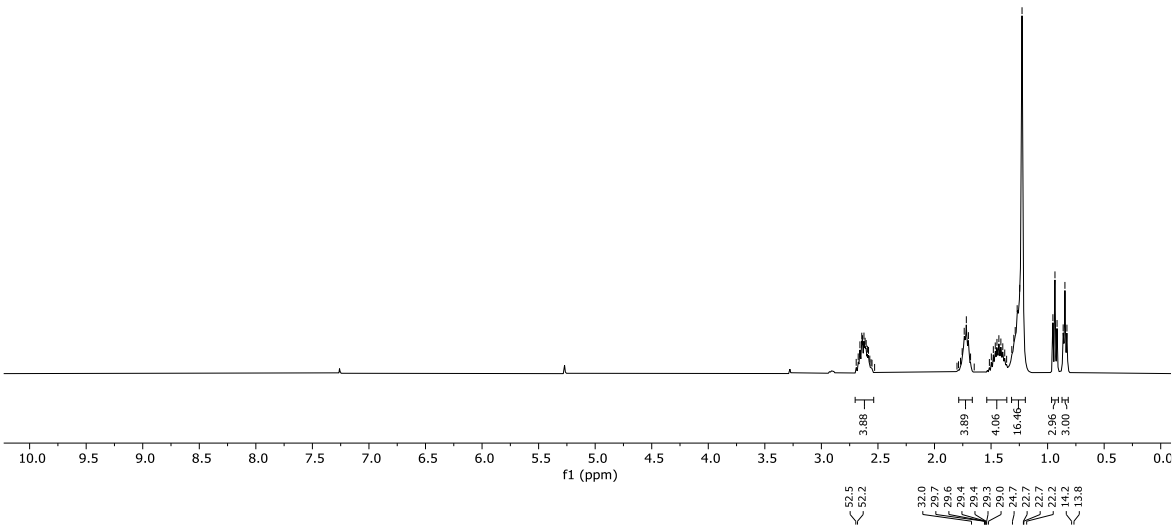
3.88
3.89
4.06
16.46
2.96
3.00
10.0
9.5
9.0
8.5
8.0
7.5
7.0
6.5
6.0
5.5
5.0
4.5
4.0
3.5
3.0
2.5
2.0
1.5
1.0
0.5
0.0
f1 (ppm)

52.5
52.2
32.0
29.7
29.6
29.4
29.4
29.3
29.0
24.7
22.7
22.7
22.2
14.2
13.8

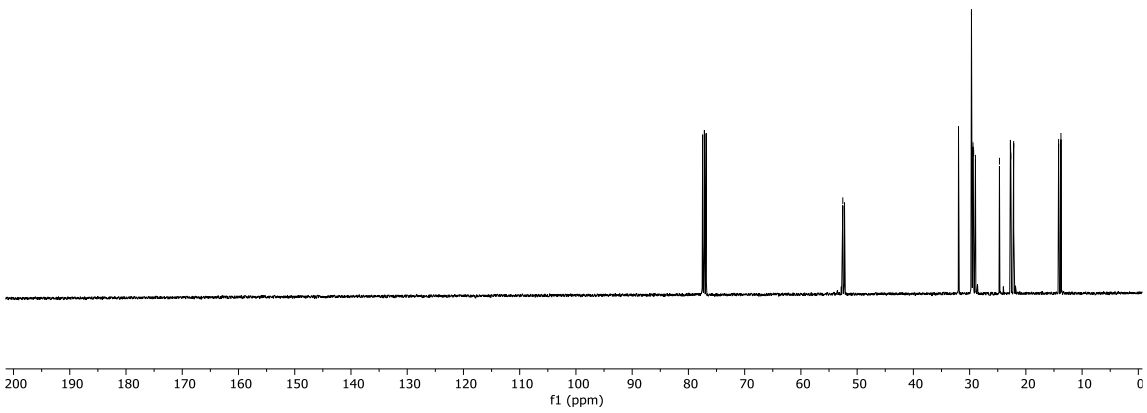
200
190
180
170
160
150
140
130
120
110
100
90
80
70
60
50
40
30
20
10
0
f1 (ppm)

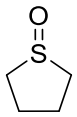

2l

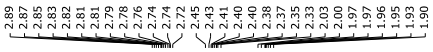
2.89
2.87
2.85
2.83
2.82
2.81
2.81
2.79
2.78
2.76
2.74
2.74
2.72
2.45
2.43
2.41
2.40
2.40
2.38
2.37
2.35
2.33
2.03
2.00
1.97
1.97
1.96
1.95
1.93
1.90

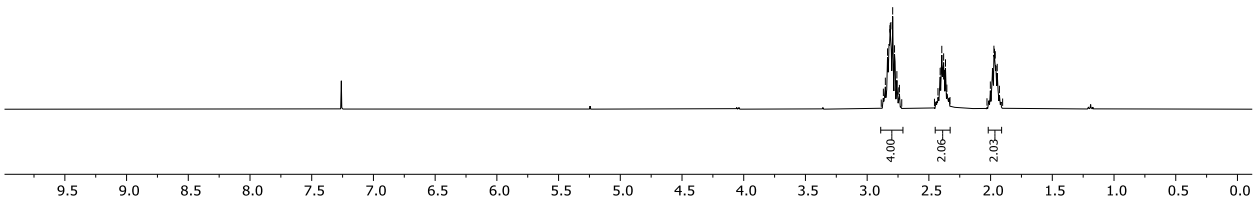
4.00
2.06
2.03
9.5
9.0
8.5
8.0
7.5
7.0
6.5
6.0
5.5
5.0
4.5
4.0
3.5
3.0
2.5
2.0
1.5
1.0
0.5
0.0

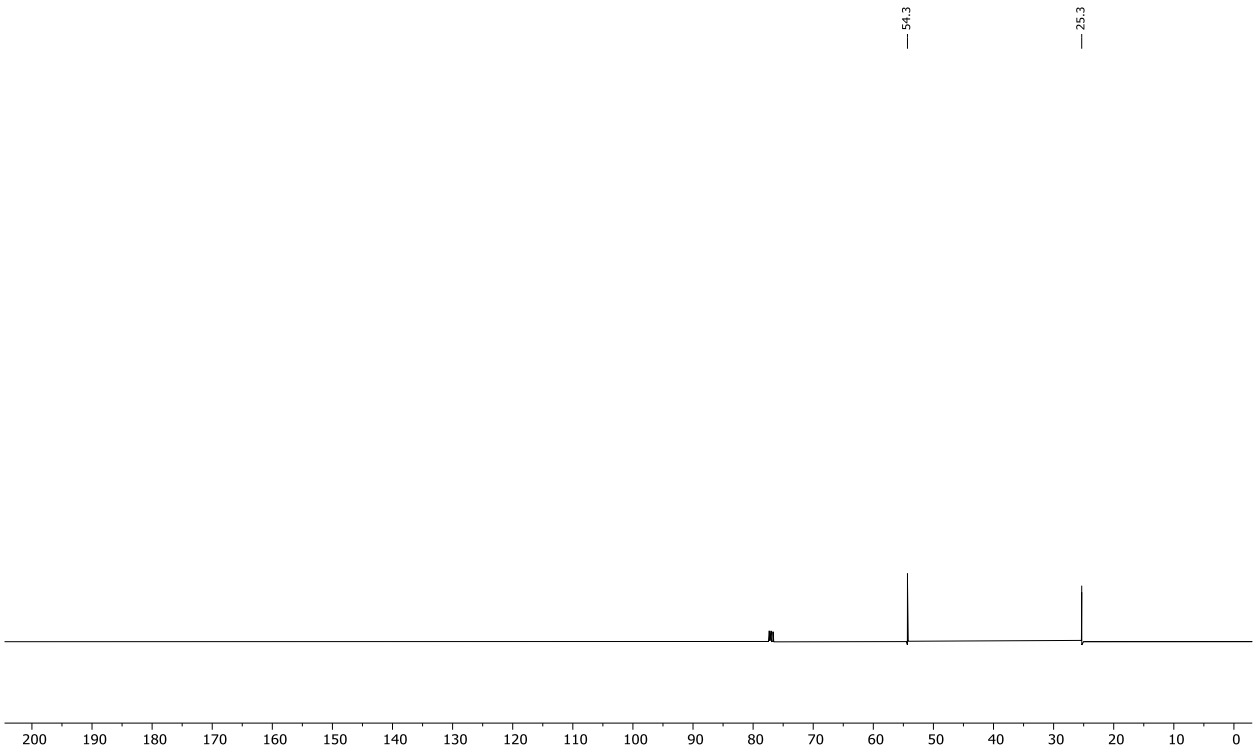
54.3
25.3
200
190
180
170
160
150
140
130
120
110
100
90
80
70
60
50
40
30
20
10
0

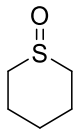
O
S

2m

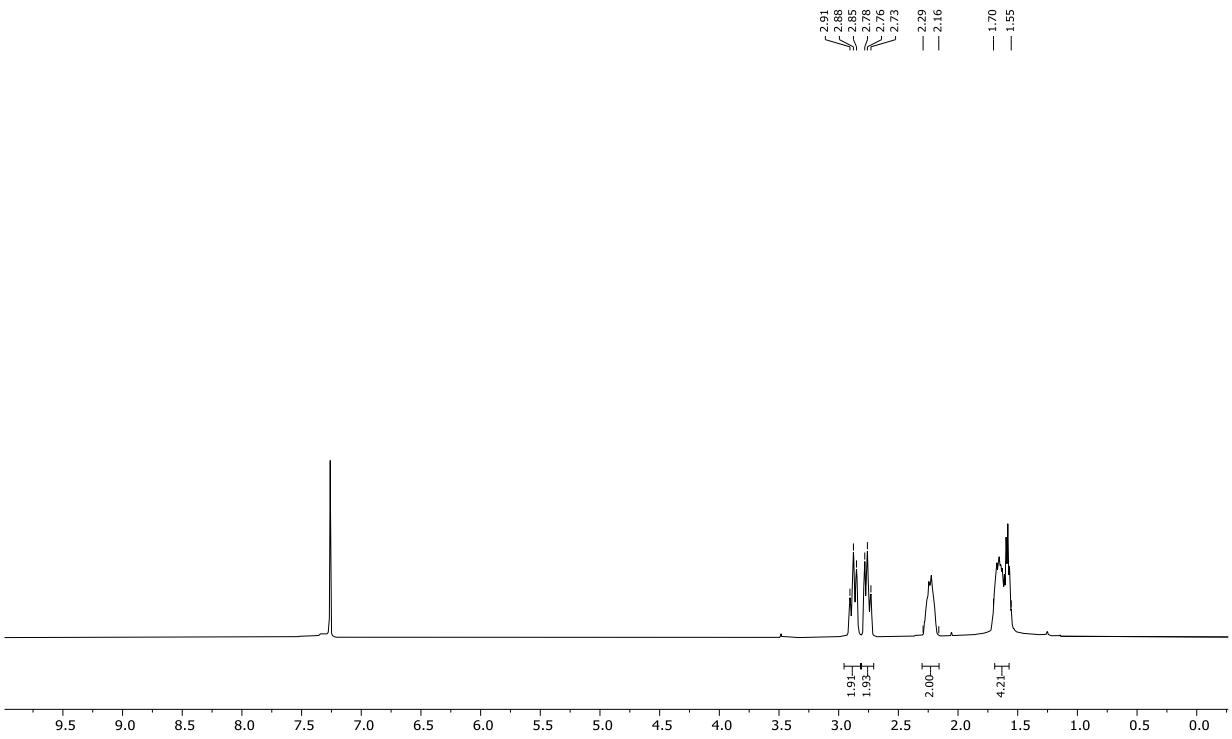
2.91
2.88
2.85
2.78
2.76
2.73
2.29
2.16
1.70
1.55
1.91
1.93
2.00
4.21
9.5 9.0 8.5 8.0 7.5 7.0 6.5 6.0 5.5 5.0 4.5 4.0 3.5 3.0 2.5 2.0 1.5 1.0 0.5 0.0

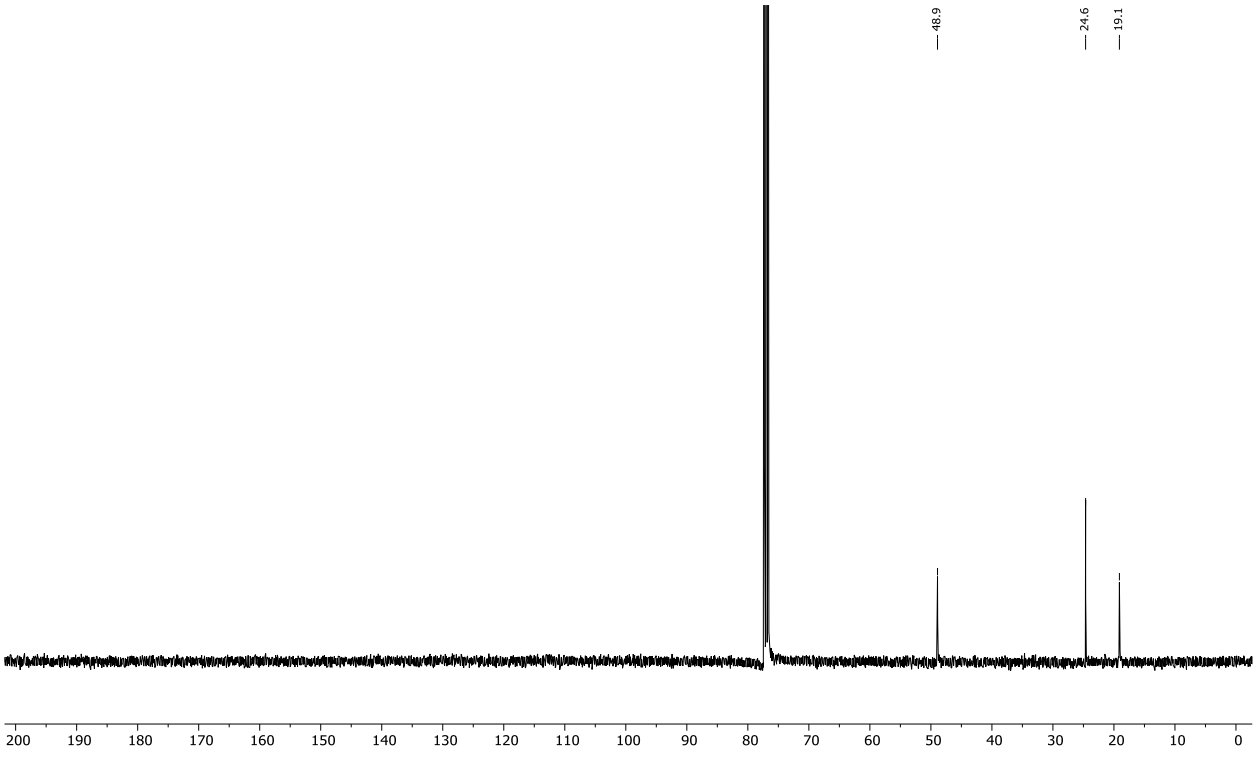
48.9
24.6
19.1
200 190 180 170 160 150 140 130 120 110 100 90 80 70 60 50 40 30 20 10 0

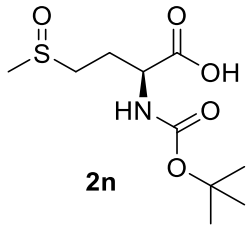

2n

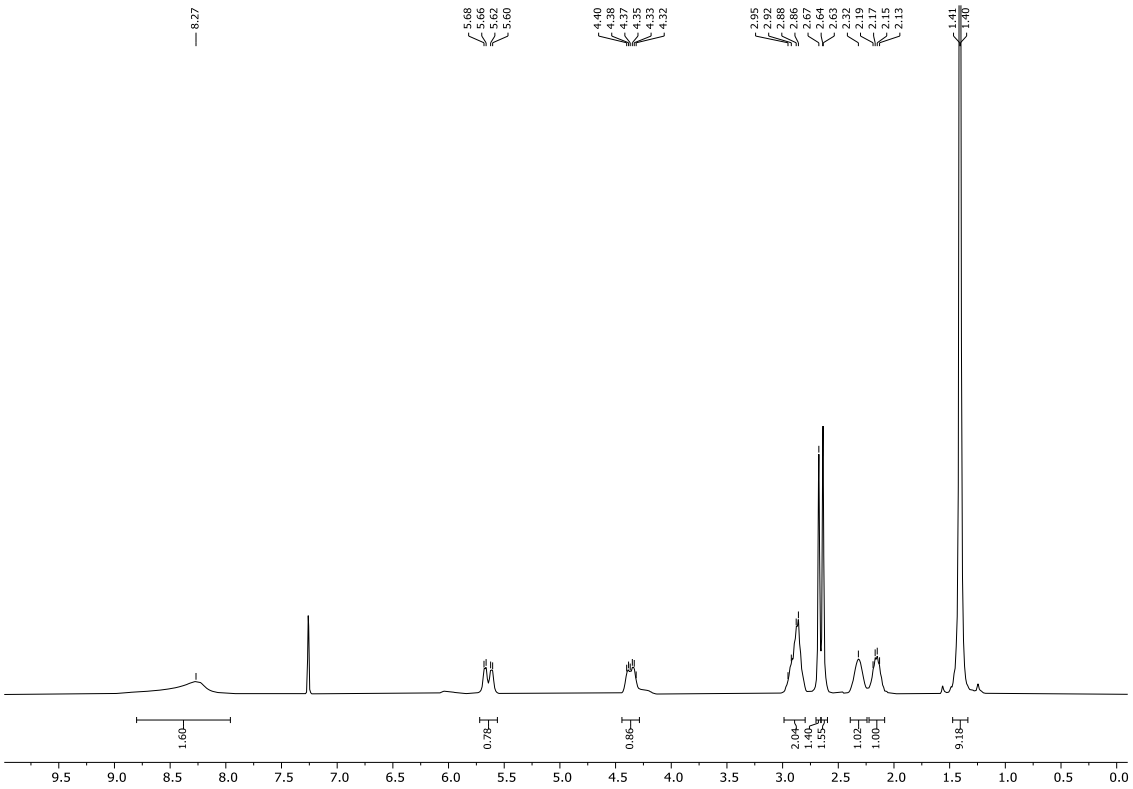
8.27
5.68
5.66
5.62
5.60
4.40
4.38
4.37
4.35
4.33
4.32
2.95
2.92
2.88
2.86
2.67
2.64
2.63
2.32
2.19
2.17
2.15
2.13
1.41
1.40
1.60
0.78
0.86
2.04
1.46
1.55
1.02
1.00
9.18

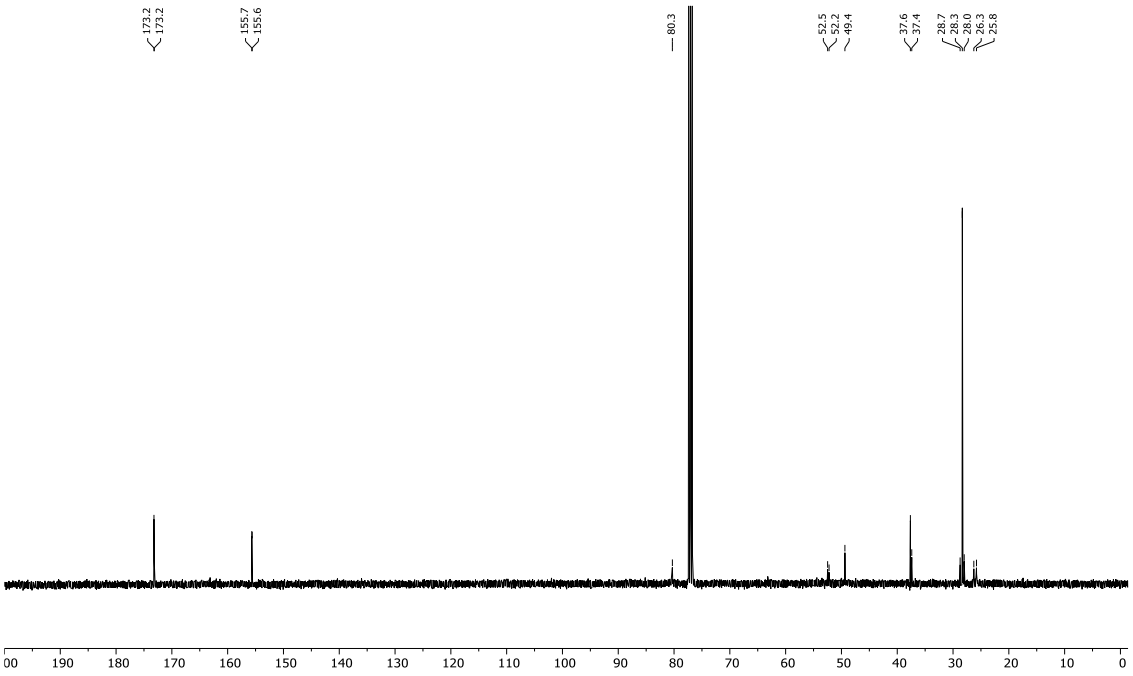
173.2
173.2
155.7
155.6
80.3
52.5
52.2
49.4
37.6
37.4
28.7
28.3
28.0
26.3
25.8

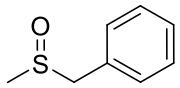

2o

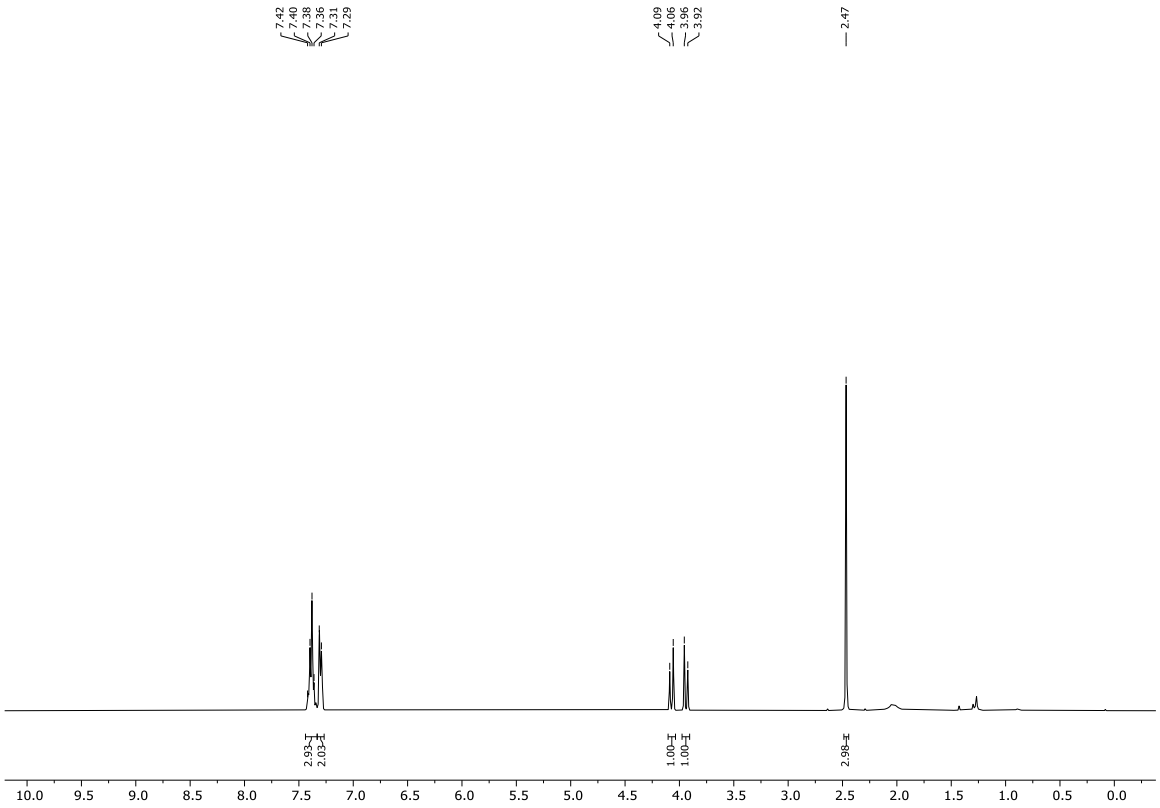
7.42
7.40
7.38
7.36
7.31
7.29
4.09
4.06
3.96
3.92
2.47
2.93
2.03
1.00
1.00
2.98
10.0 9.5 9.0 8.5 8.0 7.5 7.0 6.5 6.0 5.5 5.0 4.5 4.0 3.5 3.0 2.5 2.0 1.5 1.0 0.5 0.0

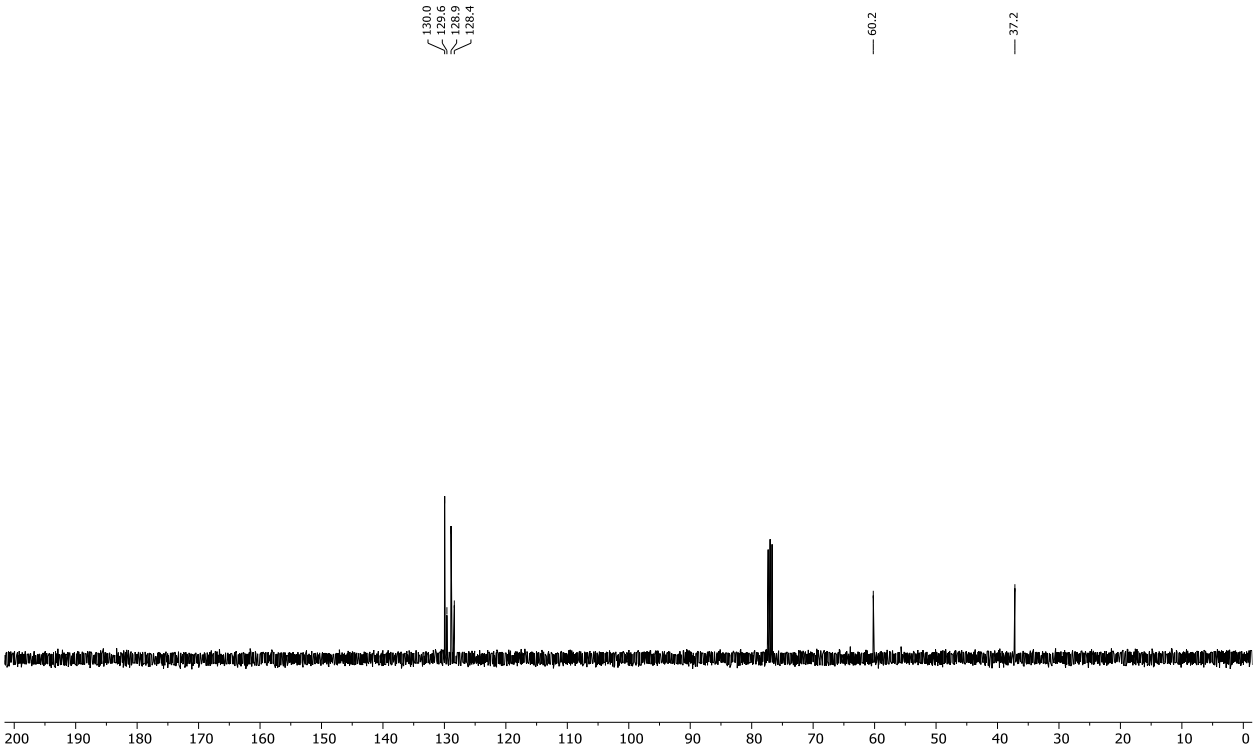
130.0
129.6
128.9
128.4
60.2
37.2
200 190 180 170 160 150 140 130 120 110 100 90 80 70 60 50 40 30 20 10 0

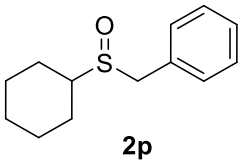

2p

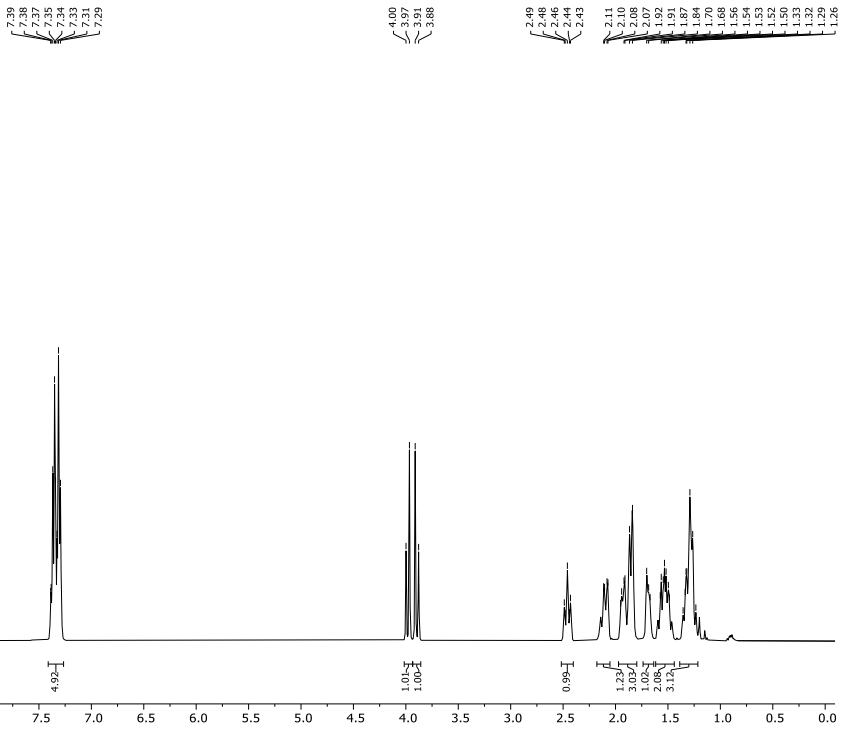

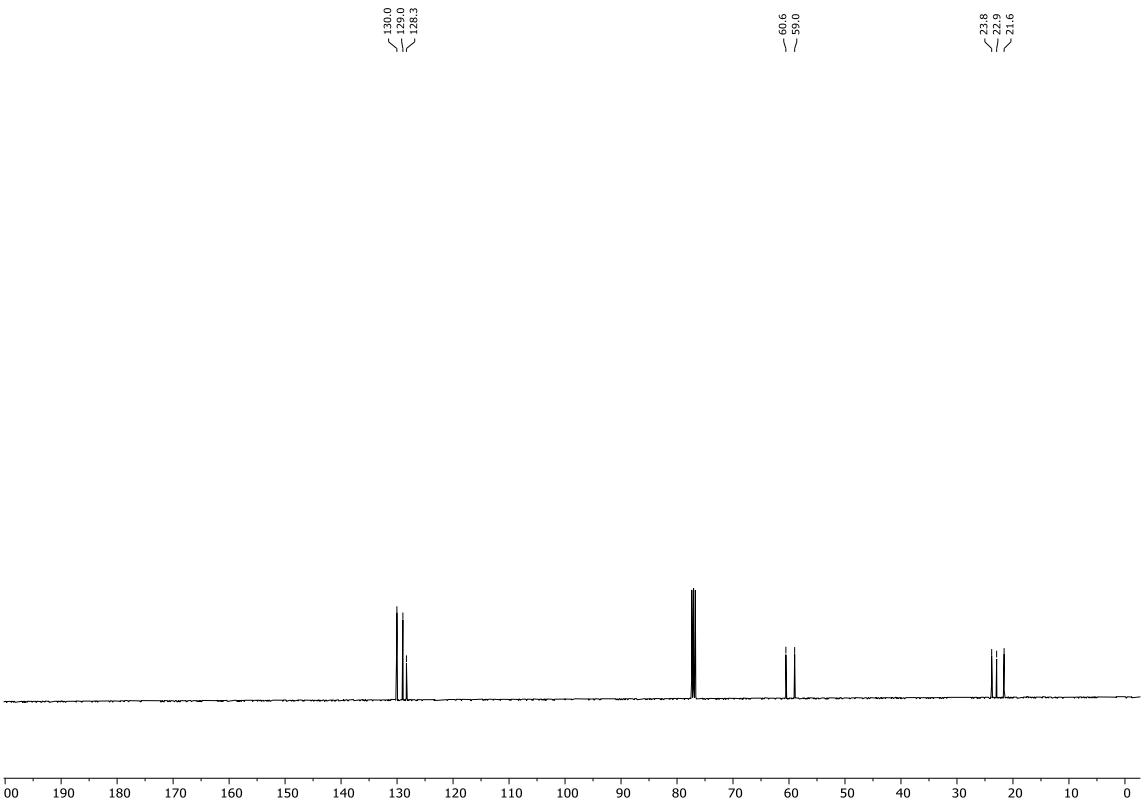

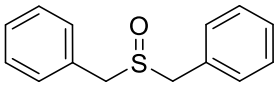

2q


7.40
7.39
7.38
7.37
7.36
7.35
7.34
7.33
7.32
7.30
7.29
7.28
7.27


3.94
3.91
3.88
3.85

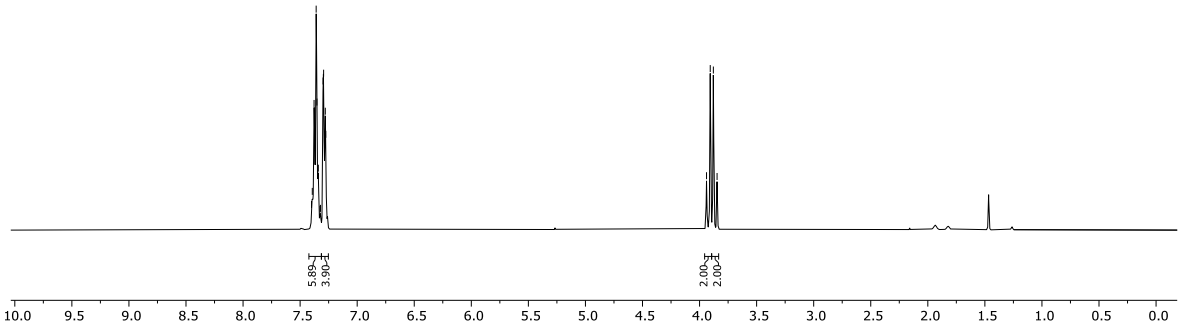
5.89
3.90
2.00
2.00
10.0
9.5
9.0
8.5
8.0
7.5
7.0
6.5
6.0
5.5
5.0
4.5
4.0
3.5
3.0
2.5
2.0
1.5
1.0
0.5
0.0


130.1
130.0
128.9
128.3

57.1

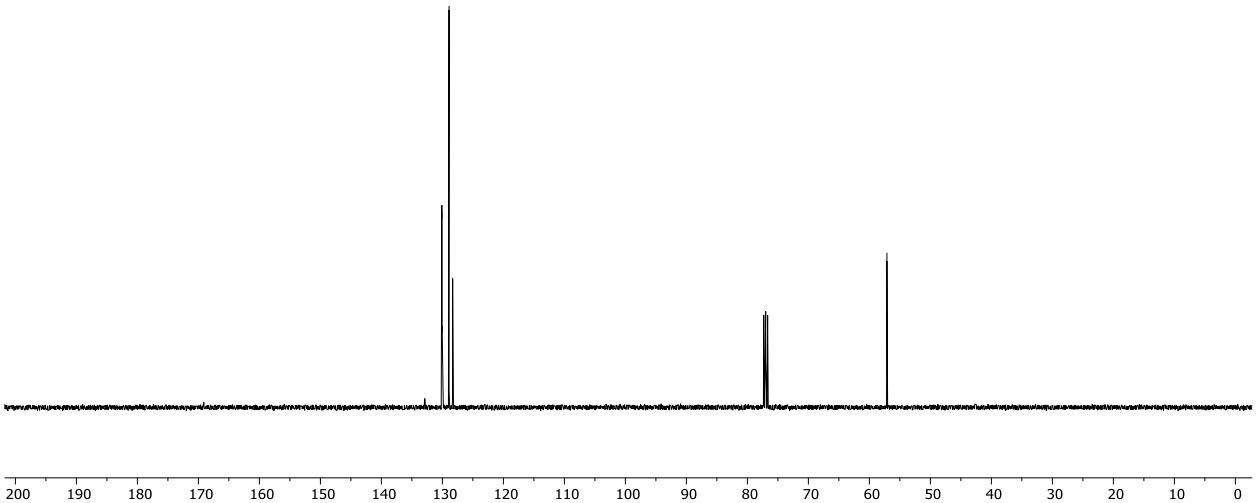
200
190
180
170
160
150
140
130
120
110
100
90
80
70
60
50
40
30
20
10
0

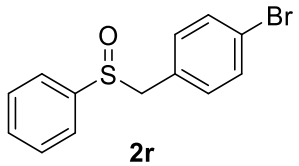
O
S
Br

2r

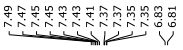
7.49
7.47
7.45
7.45
7.43
7.41
7.37
7.37
7.35
7.35
6.83
6.81
4.01
3.98
3.96
3.93

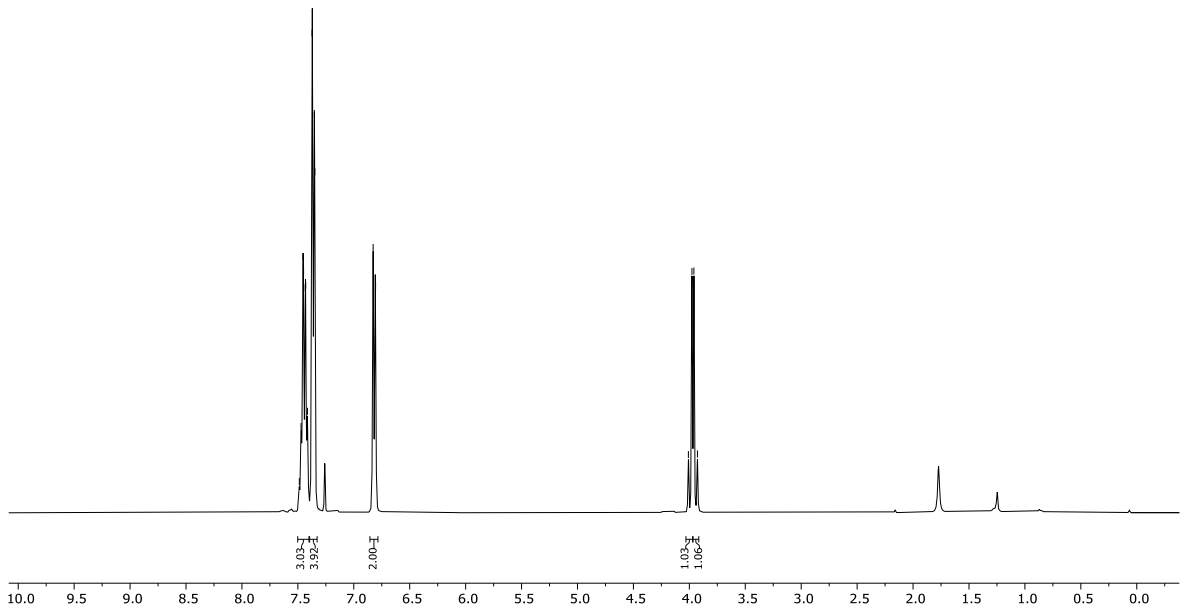
3.03
3.92
2.00
1.03
1.06
10.0
9.5
9.0
8.5
8.0
7.5
7.0
6.5
6.0
5.5
5.0
4.5
4.0
3.5
3.0
2.5
2.0
1.5
1.0
0.5
0.0

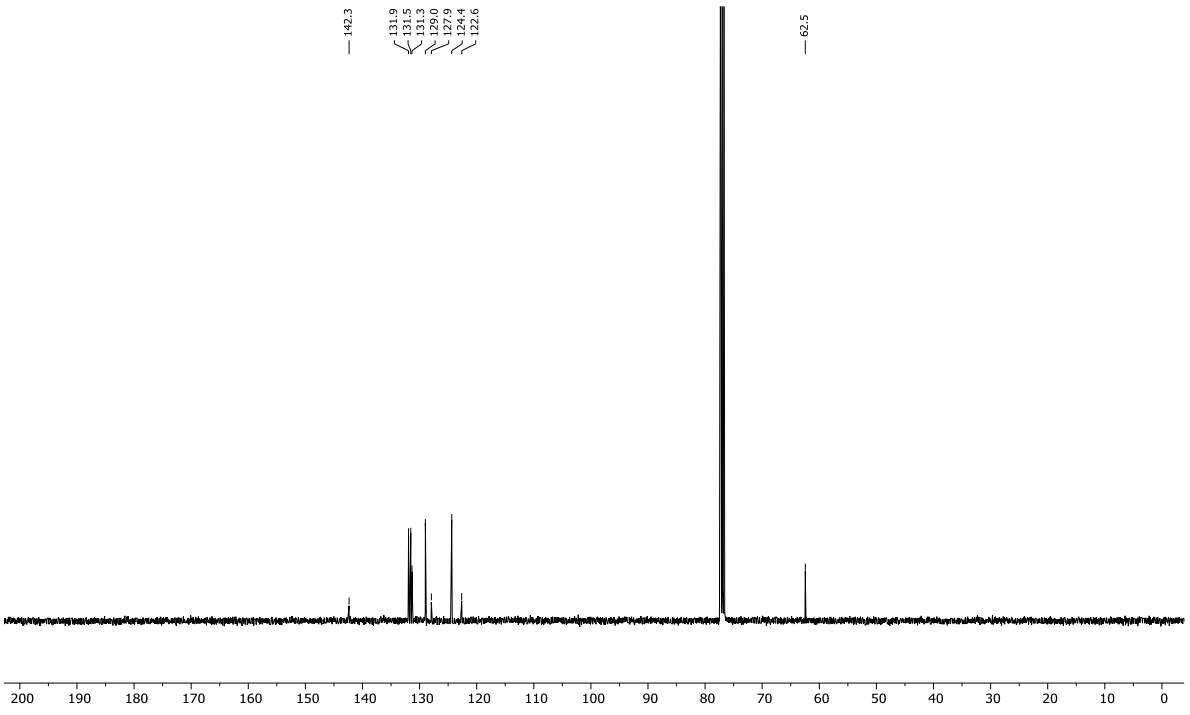
142.3
131.9
131.5
131.3
129.0
127.9
124.4
122.6
62.5
200
190
180
170
160
150
140
130
120
110
100
90
80
70
60
50
40
30
20
10
0

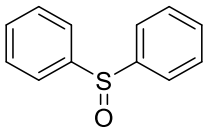

2s

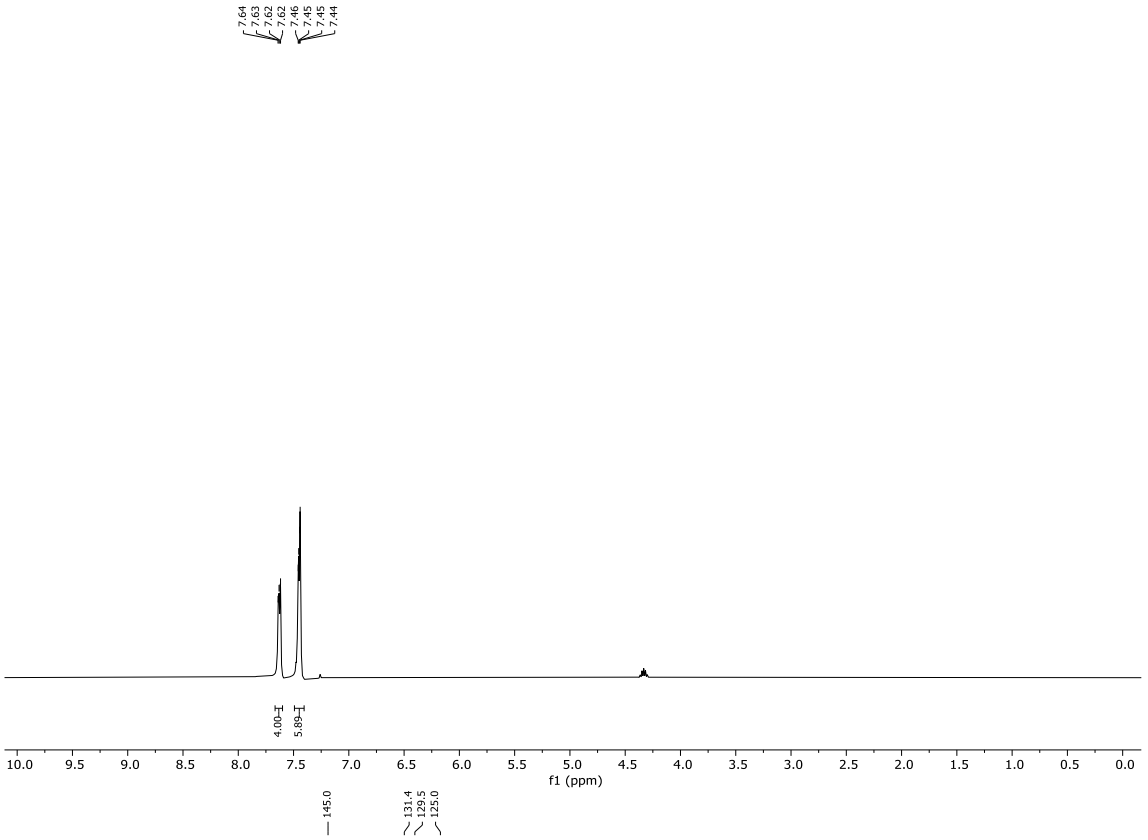
7.64
7.63
7.62
7.62
7.46
7.45
7.45
7.44
4.00
5.89
10.0 9.5 9.0 8.5 8.0 7.5 7.0 6.5 6.0 5.5 5.0 4.5 4.0 3.5 3.0 2.5 2.0 1.5 1.0 0.5 0.0
f1 (ppm)
145.0
131.4
129.5
125.0
200 190 180 170 160 150 140 130 120 110 100 90 80 70 60 50 40 30 20 10 0
f1 (ppm)

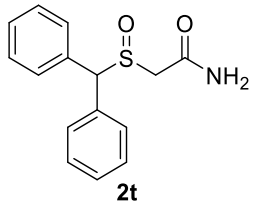
O
O
S
NH2

2t


7.51
7.49
7.45
7.43
7.41
7.39
7.38
7.36
7.05
5.62
5.20
3.51
3.47
3.12
3.08

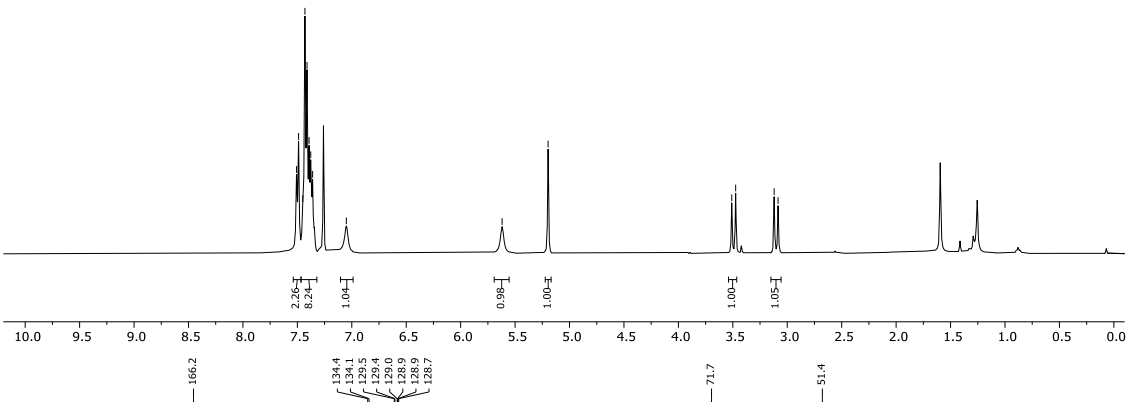
2.26
8.24
1.04
0.98
1.00
1.00
1.05
10.0
9.5
9.0
8.5
8.0
7.5
7.0
6.5
6.0
5.5
5.0
4.5
4.0
3.5
3.0
2.5
2.0
1.5
1.0
0.5
0.0

166.2
134.4
134.1
129.5
129.4
129.0
128.9
128.9
128.7
71.7
51.4

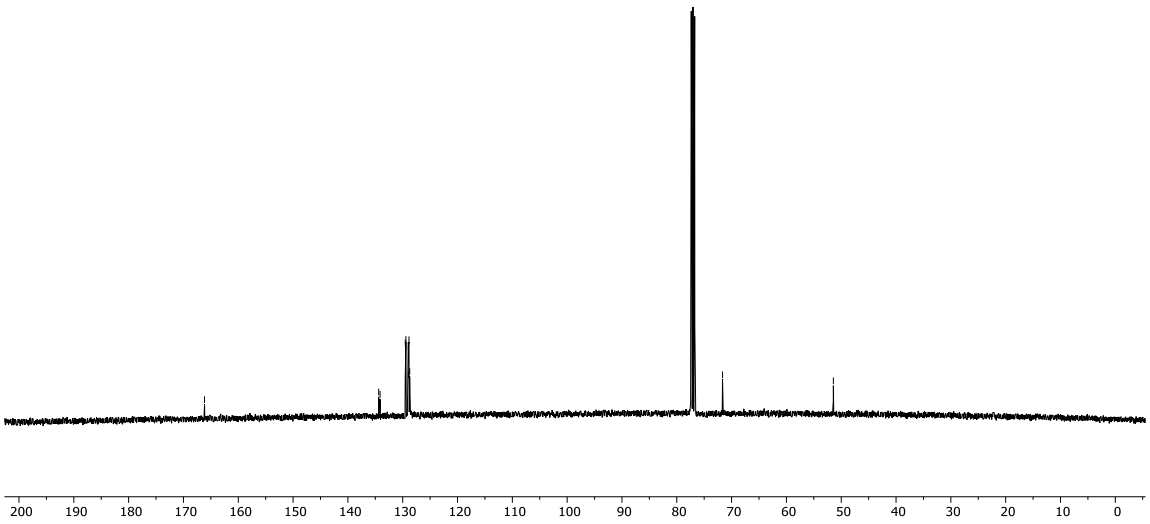
200
190
180
170
160
150
140
130
120
110
100
90
80
70
60
50
40
30
20
10
0